Renewable and Sustainable Energy Reviews 58 (2016) 267–286

Contents lists available at ScienceDirect

Renewable and Sustainable Energy Reviews

journal homepage: www.elsevier.com/locate/rser

Biomass to liquid transportation fuel via Fischer Tropsch synthesis – Technology review and current scenario

Snehesh Shivananda Ail, S. Dasappa *

Center for Sustainable Technologies, Indian Institute of Science, Bangalore 560 012, India

ARTICLE INFO

Article history:
Received 16 June 2014
Received in revised form
29 October 2015
Accepted 17 December 2015

Keywords:
Fischer Tropsch
BTL
Catalysts
FT kinetics
FT reactors
BTL economics

ABSTRACT

Current global energy scenario and the environmental deterioration aspect motivates substituting fossil fuel with a renewable energy resource – especially transport fuel. This paper reviews the current status of trending biomass to liquid (BTL) conversion processes and focuses on the technological developments in Fischer Tropsch (FT) process. FT catalysts in use, and recent understanding of FT kinetics are explored. Liquid fuels produced via FT process from biomass derived syngas promises an attractive, clean, carbon-neutral and sustainable energy source for the transportation sector. Performance of the FT process with various catalysts, operating conditions and its influence on the FT products are also presented. Experience from large scale commercial installations of FT plants, primarily utilizing coal based gasifiers, are discussed. Though biomass gasification plants exist for power generation via gas engines with power output of about 2 MW_e; there are only a few equivalent sized FT plants for biomass derived syngas. This paper discusses the recent developments in conversion of biomass to liquid (BTL) transportation fuels via FT reaction and worldwide attempts to commercialize this process. All the data presented and analysed here have been consolidated from research experiences at laboratory scale as well as from industrial systems. Economic aspects of BTL are reviewed and compared.

Contents

1. Introduction . . . 268
   1.1. Fast pyrolysis . . . 269
   1.2. Direct liquefaction . . . 269
   1.3. Transesterification of vegetable oils . . . 269
   1.4. Bio-oil from algae . . . 269
   1.5. Fischer Tropsch . . . 270
2. Technology and process background . . . 270
3. FT chemistry . . . 271
   3.1. FT reaction mechanism . . . 271
      3.1.1. Alkyl mechanism . . . 272
      3.1.2. Alkenyl mechanism . . . 272
      3.1.3. Enol mechanism . . . 272
      3.1.4. CO-insertion mechanism . . . 272
   3.2. FT catalysts . . . 272
      3.2.1. Iron catalyst . . . 273
      3.2.2. Cobalt catalyst . . . 274
   3.3. FT reactors . . . 275
      3.3.1. Low temperature FT reactor-LTFT . . . 275
      3.3.2. High temperature FT reactor-HTFT . . . 276
      3.3.3. Micro and monolithic FT reactors . . . 276
4. FT products . . . 277

* Corresponding author. Tel.: +91 80 23600536; fax: +91 80 23601692.
E-mail addresses: snehesh.s@gmail.com (S.S. Ail), dasappa@cgpl.iisc.ernet.in (S. Dasappa).

http://dx.doi.org/10.1016/j.rser.2015.12.143
1364-0321/

4.1. FT product distribution model . . . 278
4.2. Factors affecting α . . . 278
5. Biomass based FT fuels . . . 279
5.1. Environmental impacts of BTL . . . 279
5.2. BTL economy . . . 280
5.3. BTL installations . . . 281
6. Concluding observations . . . 282
Acknowledgement . . . 283
References . . . 283

1. Introduction

On one hand fossil fuel price is increasing with time and on the other hand, the cost of renewable energy based systems is gradually decreasing due to the increased available sustainable technologies relating to renewable energy. The exhaustive use of fossil fuels is one of the prime reasons for global warming leading to climate change [1]. Worldwide energy usage in the transportation sector is second only to the industrial sector in terms of gross end-use energy consumption. According to International Energy Outlook-2011 [2], the estimated fraction of global transportation fuel consumption surges from 54% in 2008 to 60% in 2035 accounting for 82% of the total increase in world liquid fuel consumption. Fig. 1 shows the increased use of all energy sources with time. Liquid fuel consumption increases at an average rate of 1% from 2008 to 2035 whereas total energy demand increases by 1.6% annually. Liquid fuels are expected to continue dominating the transportation sector despite rising prices. Global consumption of renewable sources rises by 2.8% annually, as shown in Fig. 2. Non-OECD (Organization for Economic Co-operation and Development) transportation energy use increases by 2.6% per year, compared with 0.3% per year projected for the OECD nations [2]. Current use of fossil fuels in different sectors continues to threaten global stability and sustainability. Sustainable energy sources are required due to limited availability of fossil fuel reserves and unavoidable environmental impacts of their utilization [3].

Use of renewable energy is called for primarily owing to the increased concentration of anthropogenic greenhouse gases (GHG) in the atmosphere. Emissions due to the combustion of fossil fuels for heat and electricity generation and transportation are two dominant sources of GHG emissions. These accounted for 47% and 23% respectively of total fossil fuel related CO_2 emissions in 2004 [4]. In OECD, 30% of the overall GHG emissions are from the transport sector. In the European Union (EU), average emissions for cars, in 2009, were set to 154 gCO_2/km. This limit is targeted to be further reduced, by 2020, to 95 gCO_2/km, thus counteracting the predicted GHG increase due to road transport. A fraction of this reduction could be brought about by the use of fuel efficient cars. However, the fuels in use should itself be less carbon intensive to achieve the objective [5].

Amongst the alternative energy sources, biomass plays a major role in the energy sector. The only natural, renewable carbon resource and large fraction of substitute for fossil fuels is biomass. A wide range of biomass based materials has been proposed for use, which include crop residue, agro-crops, and several tree species. These products can be burnt directly for energy and can also be processed further for conversion to liquid fuels like ethanol and diesel [6]. Thermal processes offer an effective means for the conversion of the energy content of the wood and other lignocellulosic biomass. Wood constitutes 80% or more of volatile matter and nearly 20% char can be converted to gaseous fuels. Biomass to liquid (BTL) is suggested to be a positive route to reducing the inclination towards fossil transportation fuels and is also a key to keeping the environment clean [7]. For 20% of the total liquid fuels produced from carbon neutral sources, like biomass, 15% CO_2 emissions reduction could be achieved – just by fuel replacement [8].

Processes which have been positively experimented for conversion of biomass to liquid transportation fuels include fast pyrolysis of biomass, direct liquefaction of biomass, transesterification of vegetable oils to produce diesel fuel, production of bio-ethanol from agricultural crops to blend with gasoline, production of bio-oil from algae, and most recently the FT process for conversion of biomass derived syngas to higher hydrocarbons. It is indisputable that under the current energy and environmental scenario, the global consumption of biomass derived energy which include electricity and liquid fuels would increase and most likely comprise 30% of the total energy by 2050 [9].

This paper discusses the technical details involving Fischer Tropsch process along with its recent developments and presents

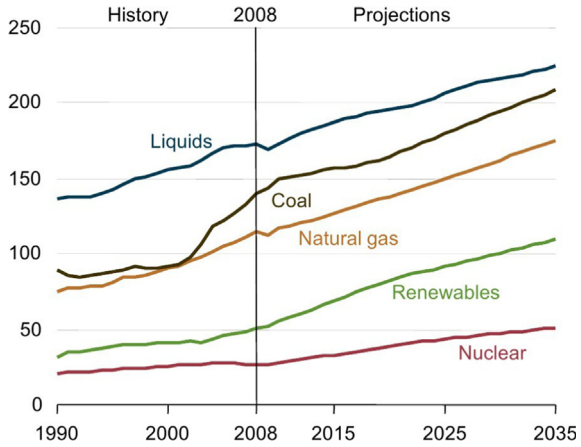

Fig. 1. World energy consumption: 1990–2035 [2].

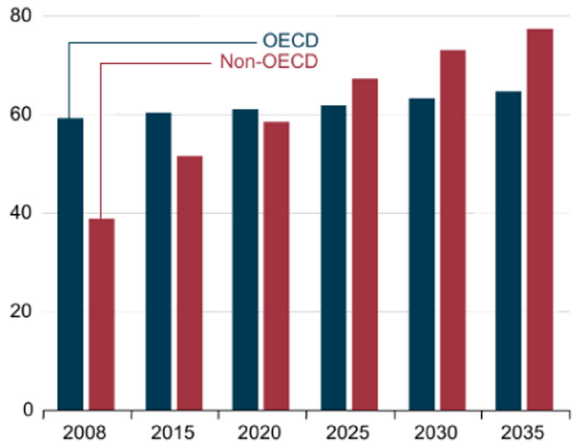

Fig. 2. World transportation energy consumption (quadrillion BTU) [2].

the current status on Biomass to Liquid fuel route. Research experiences are explored from pilot scale and large scale industrial units. This research paper distinctly summarizes the FT chemistry, catalysts, reactor configurations, product distribution, factors affecting the product selectivity, reaction kinetics, and the BTL economy along with FT plant installations.

1.1. Fast pyrolysis

Fast pyrolysis of biomass includes treating of biomass in the absence of O_2 in the temperature ranges of 450–500 °C, at heating rates of $10^3 - 10^4$ K/s with vapour residence time of one second [10–12]. The main constituent of this process, pyrolytic-oil, contains 75–80 wt% polar organics and 20–25 wt% H_2O and has a yield of 65–70 wt% of total product output along with char and gas as the by-products [11]. Even with high yields of liquids, problems with the fast pyrolysis process exist in its energy efficiency and scaling to commercial sizes [13]. One of the major disadvantages of these pyrolytic oils includes the presence of high content of O_2 and H_2O, which makes them low quality fuels compared to regular hydrocarbon fuels [14]. Also, phase separation and polymerization of these bio-oils cause great difficulty in their storage [15]. Some of the companies involved in the commercial production of bio-oil are Dynamotive and New Earth. Fast pyrolysis of biomass and its consecutive upgradation to liquid transportation fuels have several challenges that need to be addressed and only then can this technology achieve a level of commercialization for the transportation fuel industries [16].

1.2. Direct liquefaction

Direct liquefaction is a possible way of converting solid biomass material into liquid fuel under increased pressure in the presence of hydrogen and a catalyst. Dry biomass is described by the chemical formula $CH_{1.4}O_{0.7}$, liquid fuels by CH_2 and hence the chemical basis of direct liquefaction can be described by the reaction [17]

$$CH_{1.4}O_{0.7} \longrightarrow CH_2 \quad (1)$$

Hydrothermal Upgrading (HTU) is a well known process of direct liquefaction where biomass substrate is treated under extreme high pressures (150–200 bar) and temperatures in the range of 330–370 °C with a high water to biomass ratio (3:1–10:1) and residence time of 4–10 min [18]. In this case, water serves as a reactant as well as a catalyst. The products obtained are high heating value bio-crude, water soluble substances, char and gas [19]. Catalysts of various functions are added to the slurry [17]. Catalysts were used in almost all direct liquefaction processes developed. Iron based catalysts were tested for direct liquefaction processes. Iron catalysts promote pyrolysis by significantly reducing the pyrolysis activation energy. Apart from Fe based catalysts, Mo, Co and Ru catalysts have also been tested effective for the liquefaction process. SO_4^{2-}/M_xO_y solid acids also serve as active catalysts. Highly dispersed catalysts like $Mo(CO)_{6-}S$ and Ru_3CO_{12} exceptionally increase the oil productivity [20]. Presently, there are no direct liquefaction processes in commercial use [21]. The process is difficult to operate due to the presence of large amounts of oxygen that needs to be removed, before a useful fuel conforming to liquid fuel standards, being sought, results [17]. Also, the issues involved in the separation of solids from the liquid product needs to be taken care of [21]. On the economic side, the cost involved in the use of hydrogen has to be taken into account, which adds to the overall cost of operation of this process. At present, the direct liquefaction of biomass is far away from a technical and economic feasibility [17].

1.3. Transesterification of vegetable oils

Oil seed bearing trees are an ideal source of bio-diesel. Some of these trees include palm oil (oil productivity = 3.7 t/ha/yr), coconut (oil productivity = 2.2 t/ha/yr) and jatropha (oil productivity = 3.7 t/ha/yr) amongst many others [22]. The oil obtained from these seeds are subjected to the process of transesterification with methanol using NaOH or KOH dissolved in methanol as the catalyst, to produce methyl esters of straight chain fatty acids [23,24]. This process is fairly simple, and the properties of bio-diesel obtained are very similar to those of the conventional diesel fuel [25]. However, this process requires separation of a large amount of waste water produced and cleaning of catalyst and products [24]. On a larger scale, the concern always remains with the magnitude of energy input required for the production of bio-diesel from vegetable oils. A meaningful way of justifying this issue is by evaluating the energy ratio, defined by the ratio of the energy output of the end product to the fossil energy required for producing this bio-diesel. For the production of bio-diesel from soybean, this energy ratio is 3–3.5, and for palm oil the ratio is 9–9.5 [22,26]. This means that palm oil would yield three times more energy unit for every unit of fossil energy consumed as compared to soybean. To make the overall economics of this process feasible, the by-products – protein and glycerine – have to be efficiently recovered. Above all, the choice of feedstock plays a major factor in deciding the profitability of bio-diesel production [27].

1.4. Bio-oil from algae

At present, a lot of research is being conducted to establish the potential of microalgae for the production of bio-diesel. Surprisingly, oil crops like soybean, jatropha and palm oil are being used extensively for the production of bio-diesel, but the oil yield per hectare is 10–20 times higher for algal bio-diesel [28]. It is an attractive motive for several institutions and industries to invest into the research and development of production of bio-diesel from microalgae [29]. As cited by Chisti [28], oil palm would require 24% of US crop land for the production of 50% of its transportation fuel, whereas equal contribution to the transportation fuel is provided by algal biomass cultivated over just 1–3% of its total crop land. Algae contain lipids and saccharides with 2–40% of lipids/oils by weight [22]. The oil fraction in microalgae can be more than 80% by weight of dry biomass, and oil levels are mostly in the range of 20–50%. Production of microalgae is more expensive than growing oil crops [28]. Microalgae are grown in open ponds or photo-bioreactors. Though these ponds are supplied with adequate water, nutrients, CO_2, and are designed for appropriate exposure to sunlight [22,30,31], open ponds are prone to contamination by micro-organisms and extremely dependent on environmental variations(temperature, sunlight) [32]. Photo-bioreactors provide suitable conditions for algal growth but are very expensive for large scale production [22]. In the review paper by Chisti [33], the author has cited several constraints towards the commercialization of algal fuels. Some of the constraints being the provision of CO_2 from fossil fuel combustion units at the algae growth sites, the supply of nitrogen and phosphorous nutrients and drying of water for the processing of algae. Above all the best energy ratio for the production of bio-diesel from algae is estimated at 1.4 [34].

Rapid growth rate, high energy content, ability to feed on high levels of CO_2 from fossil fuel combustion and the capability of growing algae in low quality water are some of the key reasons to look towards the production of bio-diesel from microalgae, despite the several drawbacks [35,32].

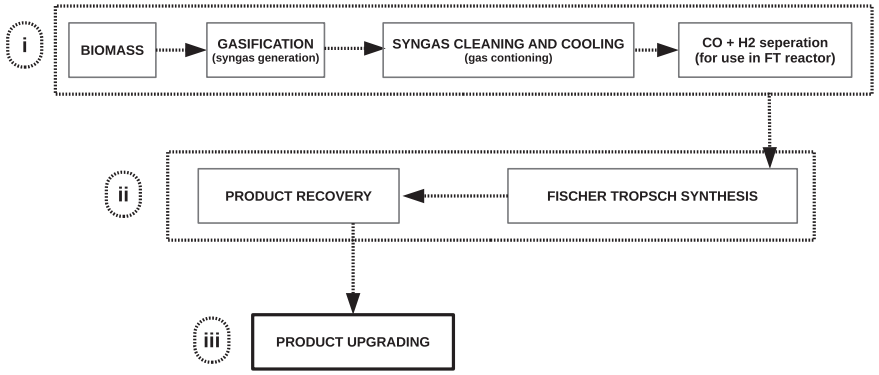

Fig. 3. FT Schematic: (i) syngas generation via biomass gasification, (ii) syngas conversion to higher hydrocarbons via FT reaction, and (iii) separation and refining of FT yield to useful products.

1.5. Fischer Tropsch

Compared to the processes considered in the prior section, FT process is a very well established, and a mastered technique for the conversion of syngas to higher hydrocarbons, especially liquid transportation fuels. An overall schematic of the FT process has been described in Fig. 3. Though all the large scale plants are either based on CH_4 reforming or coal gasification systems, biomass based FT plants should not face any major technical challenges. Biomass gasification coupled with FT process plays an assuring and an encouraging option for the production of "green" liquid fuel. Here, biomass is gasified and the bio-syngas generated is used for FT synthesis to produce long chain hydrocarbons that are converted to fractions like green diesel [36]. FT process utilizes a cobalt based or an iron based catalyst. Syngas obtained from biomass can be H_2 deficient, thus demanding a water-gas shift reactor for Co based FT synthesis. The application of Co based catalysts yields higher productivity than that of Fe based catalysts at high conversion level, whereas the productivity is approximately equal at intermediate levels of conversion, making Co as catalyst of choice [37].

Recent interest in FT synthesis has increased as a need for environmental considerations, increased use of fossil fuels and technological developments. When used in internal combustion engines the FT fuels exhibit lower emission levels compared to gasoline and diesel. This is because FT fuels are free of sulphur, consist of very few aromatics and nitrogen concentrations [38–40]. Though, at present, a lot of attention is being concentrated on BTL via FT process, a significant effort still needs to be put towards the large scale installation of this process.

2. Technology and process background

FT reaction was discovered in 1923 by Franz Fischer, Hans Tropsch, and Helmut Pichler, at Kaiser Wilhelm Institute when they reacted synthesis gas over cobalt catalyst, resulting in production of gasoline, diesel, middle and heavy distillate oils [41]. First industrial FT reactor was the Ruhrchemie atmospheric fixed bed reactor established in 1935 with a gross annual capacity of 100,000–120,000 metric tons, comprising motor gasoline, diesel fuel, lubrication oil and other chemicals. Motor gasoline constituted 72% of the total production. All plants used Co catalyst (100 Co, 5 ThO_2, 8 MgO, 200 kieselguhr), operated at medium pressure in the range of 5–15 atm and 180–200 °C, and used syngas produced by reacting coke with steam utilizing water gas shift reaction [42]. In 1955, Sasol^{TM} (South African Coal and Oil) in Secunda, South Africa, utilized circulating fluidized bed (CFB) reactors for the world's largest FT application – known as the "Synthol reactors". Reactors in operation at present are the conventional fluidized bed reactors, called Sasol Advanced Synthol (SAS) reactors. The largest version of SAS reactor has a capacity of 20,000 barrels per day. The syngas is derived from gasification of coal, and the products are mainly gasoline, diesel, LPG and some oxygenated hydrocarbon products [42]. A two-phase fluidized bed reactor, using alkalized fused iron catalyst operating at high temperatures (340 °C), was developed by Hydrocarbon Research between 1946 and 1950. This was named the Hydrocol process, using fixed fluidized bed reactor. The Hydrocol plant at Brownsville, Texas had a capacity of 350,000 t/a, operational between 1951 and 1957. However, technical problems and inexpensive crude oil availability restricted the need of GTL applications in the USA [43]. CH_4 based FT plant was established by Shell at Bintulu, Malaysia in 1993. This plant uses syngas generated from non-catalytic partial oxidation of CH_4 at pressures up to 70 bar and about 1400 °C. Four large multi-tubular reactors make use of Co based catalyst and all the reactors have a capacity of about 125,000 tons per year [44]. Shell's Pearl project at Ras Laffan, Qatar, involves identical multi-tubular fixed bed reactor and targets a production of 140,000 barrels per day [45]. Table 1 lists the commercially established FT plants.

Table 1
Commercially established FT synthesis plants [113].

Company	Site	Capacity (bpd)	Raw material	Commissioning date
Sasol	Sasolburg	2500	Coal	1955
Sasol	Secunda	85,000	Coal	1980
Sasol	Secunda	85,000	Coal	1982
MossGas	Mossel Bay	30,000	Natural gas	1992
Shell	Bintulu	12,500	Natural gas	1993
Sasol/Qatar Petroleum	Qatar	34,000	Natural gas	2006
SasolChevron	Escravos	34,000	Natural gas	2007
Shell	Qatar	140,000	Natural gas	2009

All the FT plants presented above use syngas obtained by methane reforming or coal gasification. Use of biomass based syngas for liquid fuel generation – *Biomass to Liquid* (BTL), can help curtail the economic and environmental aspects caused by the methane or coal. As of now, there are no commercial scale BTL plants, like those installed for coal to liquid (CTL) or gas to liquid (GTL). Most of the documented BTL plants are either on demonstration scale or experimental scale. Hence, minimal literature exists on BTL installations. First commercial scale BTL plant was

established by CHOREN Industries in Freiberg, Germany in 1996. It has an annual capacity of 15,000 tons of bio-fuel. Further production plants are planned in Lubmin (200,000 tons annual capacity), Dormagen and Uelzen. The liquid biofuel, *SunDiesel*, can be produced profitably in large volumes only if the production capacities are at least 100,000 tons annually. Considering this, CHOREN is establishing standard production plants with a capacity of 200,000 t/a [46].

Though there are several large scale biomass gasification systems employed for electricity generation and thermal application, it is only recently that research is concentrated on converting biomass derived syngas to higher hydrocarbons via FT process. Advanced research work on biomass gasification systems by the combustion and gasification group at the Indian Institute of Science has resulted in development of state-of-the-art biomass gasification technology utilizing variety of biomass fuel [47–49]. The open top re-burn down draft gasifier uses variety of biomass fuels with tar and particulate levels less than 5 mg/Nm^3 and exit gas composition of H_2=20%, CO=20%, CO_2=12%, CH_4=2% and balance N_2 with air as the gasification medium. The patented C^n gas cleaning and cooling system provides and ideal clean gas for direct use in FT process. Cutting edge R&D work has emerged into technology package, especially for industrial applications, resulting into large scale substitution of fossil fuels [50–52]. The experience at Indian Institute of Science has resulted in the commercialization of downdraft gasifier for power generation up to 2 MW [53–55]. More recently the work is being focused for conversion of biomass to liquid transportation fuel using syngas generated by steam-oxy gasification process. The H_2/CO ratio is maintained in the range of 2.0:1–2.3:1. Under these conditions, supported cobalt serves as an ideal catalyst in the FT reactor [56].

3. FT chemistry

FT chemistry is often regarded as the vital technological input for converting syngas to transportation fuels and other liquid products [57]. FT process converts a mixture of CO and H_2 to a range of hydrocarbons and hydrocracked into mainly diesel or gasoline of excellent quality. The process for producing liquid fuels from biomass, which integrates biomass gasification with FT synthesis, transforms a renewable feedstock into a clean fuel [58]. Hence, it can be considered as an alternative to crude oil for the production of liquid fuels – gasoline and diesel. The FT reaction is catalyzed by both iron and cobalt at pressures ranging from 10 to 60 bar and temperatures ranging from 200 to 300 °C. FT reaction is considered to be a surface polymerization reaction. The reactants, CO and H_2, adsorb and dissociate at the surface of the catalyst and react to form a chain initiator [59]. The reaction proceeds by chain propagation, chain termination and product desorption. This type of product distribution has been explained using a step-by-step addition of CH_2 monomers into the growing chain, as shown in the following equation [60]:

$$2nH_2 + nCO \longrightarrow -(CH_2)-_n + nH_2O \quad \Delta H^{o}_{250\ ^{\circ}C} = -158.5\ \text{kJ/mol}\ (n=1) \tag{2}$$

FT reaction in its simplest form is as described in Eq. (3), towards the formation of alkanes, and Eq. (4), as the formation of alkenes, where water is the prevailing oxygenated product [61].

$$(2n+1)H_2 + nCO \longrightarrow C_nH_{2n+2} + nH_2O \tag{3}$$

$$2nH_2 + nCO \longrightarrow C_nH_{2n} + nH_2O \tag{4}$$

The water-gas-shift (WGS) reaction, as shown in Eq. (5), is a reversible reaction with respect to CO and is assumed that CO_2 is essentially formed by this reaction [62]. Fe based catalysts are active WGS catalysts and, therefore, play a major role in FT chemistry when Fe is used as a catalyst.

$$CO + H_2O \longleftrightarrow CO_2 + H_2 \tag{5}$$

The overall stoichiometry of the FT process is governed by the ratio of consumption of H_2 and CO, also known as the usage ratio. Reactions 2–4 are the simplified versions of several reactions that occur during the FT process. The usage ratio varies considerably depending on the extent of the other reactions. Water gas shift (WGS) also has an impact on the usage ratio [63]. Over Fe catalysts, WGS reaction occurs concurrently with FT reaction, thereby reducing the usage ratio. This makes it possible to use syngas with H_2/CO ratio less than 2.1 [64]. Cobalt catalysts have very low activity for the WGS reaction and hence the extent of WGS reaction is negligible [65]. For cobalt catalysts, the usage ratio ranges between 2.06 and 2.16 depending on the extent of CH_4 formation, the olefin content in the longer chain hydrocarbons and slight WGS activity [63].

Considering the idealized case of biomass as a feedstock that is gasified to generate syngas and subsequently undergoes FT synthesis, the overall reaction is

$$2C + 1/2O_2 + H_2O \longrightarrow -CH_2- + CO_2 \tag{6}$$

FT synthesis yields a wide range of hydrocarbon products. Like conventional crude oil, products of FT synthesis does not refer to a single product. The composition of the FT products depends on the FT catalyst and the reaction conditions. Consequently, the FT synthesis step directly influences the product quality [66]. The formation of various FT products are steered by mechanistic and kinetic factors, and the product spectra are very different from the expected thermodynamic considerations. Under regular operating conditions, the observed C_2 and higher hydrocarbon products are produced in huge quantities compared to thermodynamic calculations [63].

3.1. FT reaction mechanism

The kinetics of the FT synthesis has been the subject of several research studies. Most kinetic studies have made use of empirical power law expressions to describe the overall reactions, but the Langmuir–Hinshelwood–Hougen–Watson (LHHW) kinetics have also been used to explain the FT mechanism. Reactants H_2 and CO adsorb dissociatively on FT catalysts, and the extent of their dissociation depends on the catalyst and reaction conditions. CO is adsorbed more strongly than H_2. The products of H_2 and CO adsorption form surface species capable of combining to form hydrocarbons by polymerization reactions [67]. Theoretical reaction mechanisms have identified distinct reactions during the polymerization steps viz. initiation, propagation and termination. Initiation is the generation of the chain-starter monomer unit from the adsorbed reactants, and propagation is the addition of these monomer units to the growing chains. Finally, termination refers to desorption of growing chains from the surface of the catalyst [68].

$$\log\left(\frac{w_i}{i}\right) = i \log\ \alpha + \log\left(\frac{(1-\alpha)^2}{\alpha}\right) \tag{7}$$

FT product distributions follow Anderson–Schultz–Flory (ASF) chain length statistics, shown in Eq. (7). Here, w_i is the product weight fraction, i refers to the hydrocarbon chain length, and α is the chain growth probability. FT reaction mechanism is expected to obey the ASF distribution, although variations may be required to account for the nature of the catalyst particles [69].

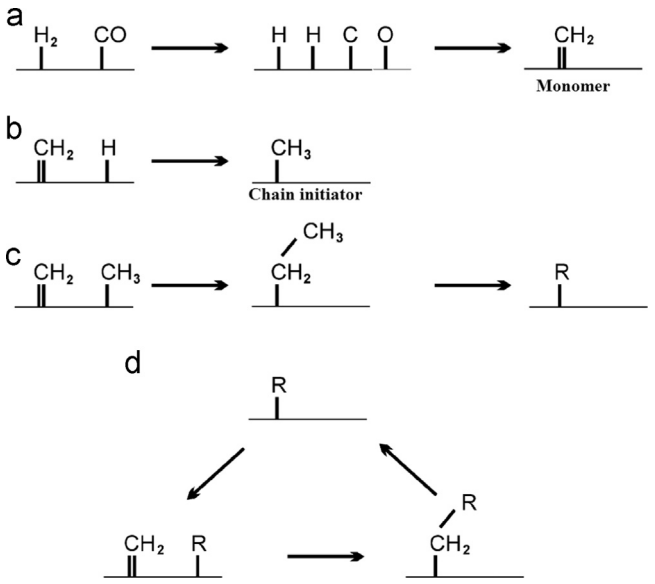

Fig. 4. Alkyl mechanism: (a) methylene formation; (b) chain initiation; (c) chain growth; and (d) propagation [175].

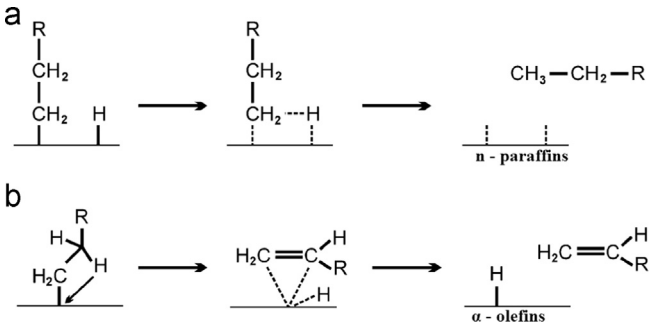

Fig. 5. Alkyl mechanism for termination of hydrocarbon chains: (a) surface hydride termination yielding alkanes and (b) β-elimination mechanism yielding α-olefins [175].

3.1.1. Alkyl mechanism

Alkyl mechanism is the most widely accepted mechanism for chain growth in FT synthesis. Chain initiation occurs using dissociative CO chemisorption, by which surface carbon and surface oxygen are generated. Surface oxygen reacts with adsorbed hydrogen yielding water or with adsorbed CO yielding CO_2. Surface C is subsequently hydrogenated yielding in a consecutive reaction CH_2 and CH_3 surface species. The CH_3 surface species is the chain initiator, and the CH_2 surface species is the monomer in this reaction scheme. Chain growth is thought to take place by successive incorporation of the CH_2 surface species. Product formation takes place by either β-hydride elimination yielding α-olefins or by hydrogen addition yielding n-paraffins as primary products [70,71]. The schematic representation of alkyl mechanism is shown in Figs. 4 and 5.

Alkyl reaction mechanism for FT process does not include the formation of branched hydrocarbons and oxygenates. Hence, an additional modification to this mechanism was incorporated to account for their formation. The alternate pathway involved the reaction of an alkylidene and a methyl surface species similar to the alkyl mechanism. The alkylidene surface species is expected to originate from a reaction between an alkyl species and methylidyne species. The branched alkyl species undergo similar desorption reactions as those proposed for n-alkyl species [72]. Experimental observations suggest the existence of branched

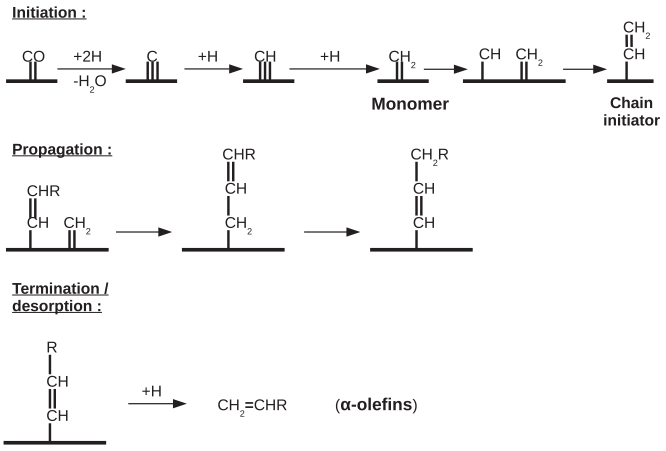

Fig. 6. Alkenyl mechanism [79].

hydrocarbons in small fractions, formed from re-adsorbed olefins, such as propene. Experiments conducted showed that the amount of branched hydrocarbons is larger than expected due to re-incorporation of re-adsorbed olefins [70]. Alternatively, to account for the formation of oxygenates, surface hydroxyl groups were known to be involved. The coupling of a surface hydroxyl group along with an alkyl group may lead to the formation of alcohols [73].

3.1.2. Alkenyl mechanism

In the alkenyl mechanism, the monomer unit is considered to be the surface methylene species [74]. Reaction initiation occurs by the generation of a surface vinyl species ($-CH=CH_2$), which is formed by the reaction of surface methyne and surface methylene species. Chain growth advances via reaction of this vinyl species with the monomer unit ($=CH_2$) to generate an allyl specie ($-CH_2CH=CH_2$). Isomerization of the allyl species results in the formation of an alkenyl specie ($-CH=CHCH_3$), which may undergo further reaction [75]. Chain termination results by reaction between surface hydrogen and the surface alkenyl species producing α-olefins [76]. This mechanism is shown in Fig. 6.

3.1.3. Enol mechanism

As per this mechanism, enol surface species is formed by hydrogenation of chemisorbed CO. Chain growth occurs through a combination of two reactions – condensation reaction between enol species and by the elimination of water. The production of branched hydrocarbons is due to the presence of a CHROH surface species [77,78]. Enol mechanism is shown in Fig. 7.

3.1.4. CO-insertion mechanism

In this mechanism, the chemisorbed CO itself is proposed to be the monomer. Surface methyl species is considered to be the chain initiator. CO-insertion mechanism is shown in Fig. 8. CO-insertion in the metal alkyl bond results in the formation of a surface acyl species causing the chain to grow. Oxygen removal from the surface species results in the generation of enlarged alkyl species. Chain termination takes place similar to the alkyl mechanism, and the presence of oxygenated compounds could lead the termination steps to form of aldehydes and alcohols [79].

Table 2 summarizes various FT mechanisms.

3.2. FT catalysts

An ideal FT catalyst should possess a high hydrogenation activity to catalyze the hydrogenation of CO to higher hydrocarbons. There are four transition metals that possess sufficiently

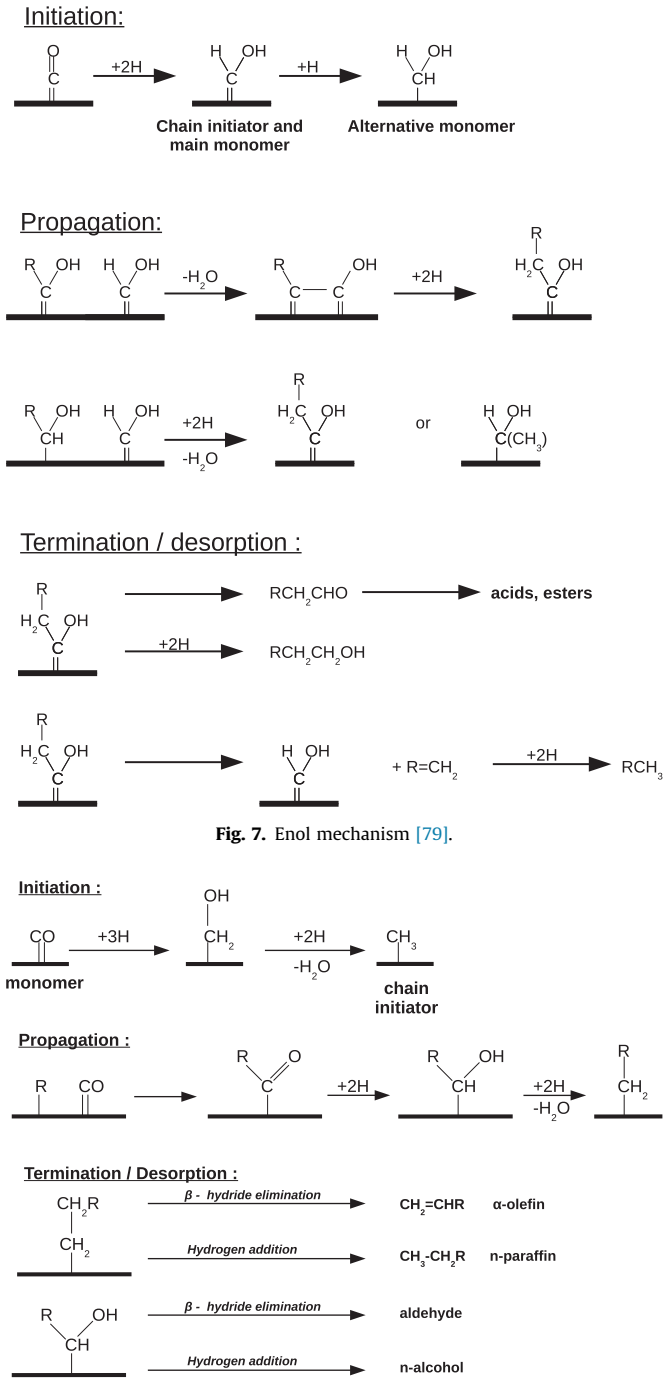

Fig. 7. Enol mechanism [79].

Fig. 8. CO-insertion mechanism [79].

high hydrogenation activity for use in the FT synthesis process – iron, cobalt, nickel and ruthenium [80]. Iron catalysts are the most common catalysts, primarily due to easy availability and low costs in comparison to other metals. Ruthenium has the highest activity for the FT reaction but is an expensive catalyst compared to Fe and Co [63]. Nickel too has got very high activity for hydrogenation. However, it produces much more methane than Fe or Co. Also, it forms volatile carbonyl resulting in continuous loss of the metal at the temperatures and pressures at which practical FT plants operate. Hence, Fe and Co are the only two ideal metals that can be used for practical application of FT synthesis. Overall, as far as the commercially viable metals are concerned, Co appears to be more active than Fe. The FT turnover rates on Co catalysts are significantly larger than on Fe catalysts [81].

Intrinsic rates of FT reaction on the catalyst surface, and the rates of diffusion of reactants and products across the porous catalyst particles dictate the overall reaction rates. In particular, the diffusion rates depend on the porosity and pore sizes, catalyst particle size, species concentration, and on the presence of higher hydrocarbons, especially liquid waxes, within the catalyst particles. As seen in the Thiele–Wheeler plot, shown in Fig. 9, the catalyst effectiveness drops less than one as the Thiele modulus, ϕ, rises above unity. Clearly, intra-particle diffusion plays a crucial factor for FT catalyst particle with diameters relatively greater than 0.5 mm, thus making intra-particle diffusion a critical parameter for consideration while selecting catalyst particle size and shape for a fixed-bed FT process [82].

3.2.1. *Iron catalyst*

Fe catalyst, owing to its relatively low costs and easy availability, is the most common catalysts used for the FT process. Initial FT processes employed catalysts that were synthesized by precipitation method [83]. Zimmerman et al. synthesized catalyst using continuous precipitation method. An aqueous solution of

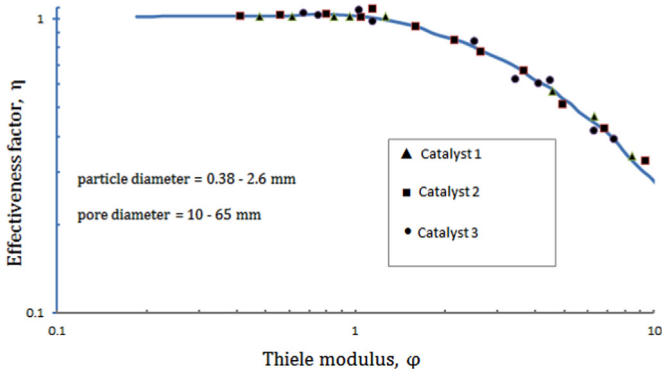

Fig. 9. Catalyst effectiveness ϕ as a function of the Thiele modulus for various cobalt and iron catalysts. H_2/CO molar ratio 2, P=2.1 MPa, T=473–513 K [82].

Table 2
Summarizing FT mechanism.

Mechanism	Monomer species	Chain initiator	Products	Remarks
Alkyl	⊨CH2	⊢CH3	α-olefins, n-paraffins	Inadequate to account formation of branched HC and oxygenates
Akenyl	⊨CH2	⊢CH=CH2	α-olefins	Only explains formation of α-olefins as primary products
Enol	⊨C(H)(OH)	⊨C(CH3)(OH)	Aldehydes, alcohols, α-olefins	Unable to explain formation of n-paraffins
CO-insertion	⊨CO	⊢CH3	α-olefin, n-paraffin, aldehyde, alcohol	Primary pathway for formation of oxygenated FT compounds

iron and copper nitrate was used to prepare catalyst precursor at the desired Fe/Cu ratio using aqueous ammonia. The catalyst was dried and promoted with potassium using $KHCO_3$ via incipient wetness impregnation method. Finally, the catalyst was dried at 120 °C for 16 h in a vacuum oven. This catalyst had composition of 100 Fe/0.3 Cu/0.2 K (by weight) [84]. Wilfried et al. synthesized precipitated iron–silica catalyst by continuous co-precipitation in a stirred tank reactor. The catalyst had atomic ratio composition of 100 Fe/4.6 Si. Thereafter, alkali (Li, Na, K, Rb and Cs) was incorporated into the catalyst by incipient wetness impregnation method using an aqueous alkali carbonate solution such that alkali/iron atomic ratio of 1.44/100 was obtained [85].

During the prevailing reaction conditions, Fe catalyst can exist in the form of magnetite, α-Fe, or in the form of Fe-carbide. The existence of these phases during the FT reaction have a direct consequence on the FT product distribution [86]. It is necessary to reduce the Fe catalyst prior to use in the FT reactor. The need to reduce the catalyst is to achieve active catalysts with high metallic surface areas. The extent of reduction and method of reduction intensely influences the FT selectivity. Reduction with H_2 at 300 °C produces more active catalysts than reduction with syngas at 230 °C. However, the catalyst reduced with H_2 has a lower wax selectivity [83]. Fe catalyst can be activated by reducing, in an environment containing CO, syngas or H_2. Reduced activity is observed for catalysts pre-treated in syngas as compared to the catalysts that are pre-treated in CO. Fig. 10 shows reduced CO conversion when lower H_2/CO ratio syngas is used for activation of Fe catalyst [87]. Sasol uses H_2 for reducing its promoted Fe catalyst. Reduction in H_2 results in a zero-valent state, but during FT synthesis process the zero-valent metallic Fe gets converted to a carbide phase or a mixture of Fe-carbides, sometimes also leading to the formation of magnetite. Some researchers claim iron carbide to be the most active phase and some assert Fe_3O_4 to be the active phase for FT synthesis [88,89].

Promoters are added to Fe catalyst for increased activity and improved stability. The addition of potassium enhances CO chemisorption and reduces H_2 chemisorption due to electron donating nature of potassium to iron, thus aiding CO chemisorption since CO readily accepts an electron from Fe. Furthermore, hydrogen donates electrons to Fe, and the existence of electron-donating alkali weakens the iron-hydrogen bond, boosting the Fe–C bond and reducing the strength of the C–O and Fe–H bonds [90,91]. Tao et al. [92] used manganese as a promoter for their Fe catalyst in a slurry reactor. They concluded that initial FT synthesis activity reduced with increased Mn content due to weak carburization. However, Mn was able to restrict the re-oxidation of iron carbides to Fe_3O_4 and augment additional carburization of the catalyst, maintaining stability during FT reaction. At the same time, Mn promotion restricted CH_4 formation and increased light olefin selectivity.

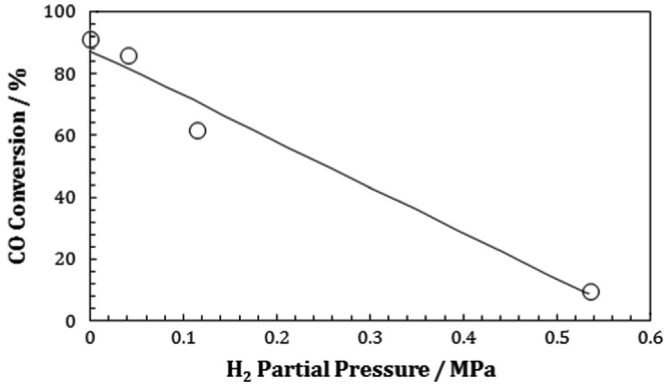

Fig. 10. CO conversion for Fe catalyst activated in syngas with varying H_2 partial pressures; catalyst: 100 Fe/3.6 Si/0.7 K; FTS conditions: 270 °C, 1.31 MPa, H_2: CO = 0.7:3.1 [87].

With Fe catalysts, FT reactions exist over wide temperature ranges(~210–350 °C). Schulz et al. further claimed that the active Fe catalyst for FT synthesis is "constructed" in several stages of "self-organization", during which conversion, selectivity, catalyst composition and structure change, concluding that Fe in its zero valent state is not the active phase. FT activity develops when iron carbide are formed [93]. Use of Fe catalysts produces broad range of hydrocarbon products including paraffins and olefins. The products vary from fractions of methane to high molecular weight waxes. Fe catalysts show varying WGS activities and, in some cases, leading to rejection of 30–50% carbon feed in as CO_2. α-olefins are the primary products formed over iron catalysts. However, olefins can undergo secondary reactions resulting in isomerization or hydrogenation [94]. In experiments conducted by Rao Pendyala et al. [95], the effect of the addition of varying amounts of water on selectivity and activity of alkali promoted precipitated Fe catalysts was investigated. Increased addition of water in feed gas reduced the selectivity to C_{5+} hydrocarbons due to increased WGS activity and simultaneously increased the selectivity to oxygenates. Fe catalysts are designed for operations in high temperature FT reactions (~340 °C), for the production of low molecular weight olefinic hydrocarbons, and for operations at low reaction temperatures (~230 °C), for the production of paraffin waxes, which can be further hydrocracked for producing high quality diesel [96].

3.2.2. Cobalt catalyst

Cobalt catalysts possess high activity with 60–70% conversion in a single pass, along with high selectivity and stability in the synthesis of linear hydrocarbons. Cobalt catalysts exhibit good resistance to attrition in slurry bubble column reactors. Due to negligible WGS activity over cobalt catalysts, there is no effect of water on CO conversion. Excessive CH_4 formation at higher temperatures over cobalt catalysts restricts its use to lower temperatures [80]. Cobalt catalysts show high methane and C_2–C_4 selectivities at temperatures above 250 °C. At temperatures below 200 °C, CH_4 selectivities are less than 15% along with low metal- and site-time yields. Another unfavourable aspect of cobalt catalyst is the difficulty in the regeneration of deactivated catalysts, which requires sequential hydrogen and steam treatments or a solvent wash [97]. Relative high costs of cobalt based catalysts make the study of catalyst deactivation a major challenge. The synthesized catalysts need to have apart from good activity and selectivity, long life. Oxidation of cobalt to its oxide form by water and CO_2 is the main cause of deactivation of the catalyst though long term effect on cobalt based catalysts due to CO_2 is very small [98].

Factors that govern the catalyst design for FT synthesis are its productivity and its selectivity to C_{5+} hydrocarbons. High cobalt concentrations and high site density catalysts can be synthesized from carefully steered reduction reaction of nitrate precursors added via melt or aqueous impregnation methods. FT synthesis turnover rates are unaffected by the choice of support and cobalt dispersion within the dispersion ranges of 0.01–0.12, at typical FT reaction conditions [99]. To achieve low metal loading and maximize the available surface area, cobalt is dispersed on stable supports such as Al_2O_3, SiO_2 or TiO_2 with cobalt metal loading in the range of 10–30 g per 100 g of support [44]. FT plants in German prepared catalysts by co-precipitating nitrates of cobalt and thorium with a basic solution in the presence of kieselguhr having catalyst composition with a mass ratio of 100 Co/18 ThO_2/100 kieselguhr [83]. Snehesh and Dasappa [100] have described a novel method for the synthesis of SiO_2 supported cobalt catalyst using solution impregnation combustion synthesis (CS). The CS

synthesized catalysts had higher metal dispersion, smaller crystallite sizes and homogeneous Co deposition over SiO_2 pellets, compared to the catalysts synthesized using conventional impregnation method. Though few researchers have utilized solution combustion method for synthesizing powdered Co catalysts for use in slurry phase processes [101–103], Snehesh and Dasappa [100] developed a technique to synthesize Co nanocrystals on SiO_2 extrudates for direct use in fixed bed reactors.

The addition of copper reduces the temperature required to reduce cobalt oxide to metallic cobalt, which is the active phase for FT synthesis. But, the presence of copper decreases the cobalt catalyst activity. Hence, alternative promoters need to be used [83]. Noble metal promoters such as Pt, Ru and Re are often added to cobalt catalysts. These metals catalyse cobalt reduction by H_2 spillover from the promoter surface, thus reducing the temperature at which reduction occurs. Also, textural promoters are used to increase dispersion, improve attrition resistance, build up a sulphur tolerance or electronically modify the active metal site. These metals include Zr, La, B and K [104]. Experiments by Thiessen et al. [105] showed considerable higher C_{5+} selectivity, lower methane selectivity and higher olefin to paraffin ratio, compared to an un-promoted catalyst for Mn promoted carbon nanotubes supported cobalt catalysts. Table 3 compares some of the salient features of cobalt and iron based FT catalysts [106–110].

3.3. FT reactors

The strong relationship between FT catalyst and catalytic reactors has resulted in the design of various types of heterogeneous gas solid catalytic vapour phase reactors for such a multi-product reaction system. Table 4 lists prominent features of some initially developed FT reactors [111].

Most common reactors include multi-tubular fixed-bed reactor, the slurry reactor, three phase fluidized bed reactor, fluidized bed reactor, and circulating fluidized-bed reactor [82]. Currently, there are two operating modes for the FT reactors – high temperature mode (300–350 °C) and low temperature mode (200–240 °C). Iron catalysts are employed in high temperature mode for the synthesis of gasoline and linear low molecular olefins. On the other hand, low temperature processes utilize either iron or cobalt catalyst for the production of high molecular mass linear waxes. In case of fluidized bed reactors, the bed being more isothermal compared to fixed bed reactors, it can be operated in the temperature range of 320–350 °C which is 100 °C higher than the operating temperature range used with the tubular fixed bed reactor and slurry phase reactors [112]. Fig. 11 shows the type of reactors in commercial use.

3.3.1. Low temperature FT reactor-LTFT

Modern FT processes employ low temperature processes for the production of liquid fuels. In these reactors synthesis gas, liquid products, and solid catalysts co-exist. The primary aim of any FT reactor is to remove the large heat of reaction produced during the FT process and maintain uniform temperature profile within the catalyst bed [113,114]. Guettel et al. [113] grouped the various possibilities for LTFT reactors as follows:

1. cooling with internal tubes, where coolant fluid circulates in the tubes, within suspended or fixed bed reactors.
2. external cooling – this is enabled by recycling of gas or liquid into the catalyst bed.
3. direct cooling by dispersing the feed of inlet synthesis gas in stacked fixed bed reactors.

Most common type of fixed bed reactor is a multi-tubular reactor, with the catalyst placed within the tubes and cooling medium on the shell side. The short span between the catalyst particles and the tube walls and high gas linear velocities significantly augments heat transfer from the catalyst particles to the cooling medium, maintaining steady FT temperature range. Syngas recycling aids in improved heat transfer and also in increased overall conversion. Similarly, recycling of liquid hydrocarbon products also enhances the temperature profile in the fixed bed reactors [112]. Due to the similarity in behaviour of the parallel tubes in multi-tubular reactors they are easy to handle and design [113]. Some of the other advantages of the multi-tubular fixed bed reactors include the absence of catalyst–wax separator since the heavy wax products trickle down the bed and gets collected in the receiver pot. Most importantly, the behaviour of large scale reactors can be predicted accurately based on the performance of pilot scale plants [115]. Limitations of the fixed bed FT reactor include the pressure drop constraint; and hence catalysts in fixed bed reactors have diameters greater than about 1 mm. Intraparticle diffusion plays limiting factor for the overall reaction rate for catalysts with sizes greater than 1 mm. Consequently, intraparticle diffusion is an important factor that needs to be accounted for while choosing catalyst particle size and shape for a fixed-bed FT process [115].

Table 3
Comparison of some salient features of cobalt and iron FT catalysts.

Parameter	Co catalyst	Fe catalyst
Operating temperature	190–240 °C Used only in LTFT reactors High temperature increases CH_4 selectivity and causes catalyst deactivation	200–350 °C. Operates both in HTFT and LTFT reactors
Feed gas	Syngas with H_2:CO ratio in the range of 2.0–2.3, due to very low WGS activity	Flexible H_2:CO ratio in the range 0.5–2.5, due to high WGS activity
Activity	More active at higher CO conversions i.e., lower space velocities	More active than Co at higher space velocities
Product spectrum	Primary products are n-paraffins with marginal production of α-olefins Higher paraffin/olefin ratio α=0.85–0.92	Primary products are n-paraffins with considerable production of α-olefins Lower paraffin/olefin ratio α=0.65–0.92
Operating plants	Shell Middle Distillate Synthesis, Oryx-GTL facility-Sasol	Sasol Slurry process (LTFT), Sasol-SAS (HTFT), Mossgass facility
Promoters	Noble metals (Ru, Rh, Pt, Pd); Oxide promoters (ZrO_2, La_2O_3, CeO_2)	Alkali metals (Li, Na, K, Rb, Ca)
Life & cost	Longer life time, more expensive	Lower life time, less expensive

Table 4
FT reactors [111].

Type of reactor	Status	Structural features	Operating temp (°C)	Approx. heat transfer coefficient (kcal/m^2/h/°C)
Old fixed bed (German)	Industrial scale (obsolete)	Shell & double tube (concentric)	220–260	30
Improved fixed bed (Arge)	Commercial	Shell & tube	220–260	150
Multi bed	Pilot Scale	Shell & tube and tray		NA
Tubular-cum tray	Pilot scale	Shell & tube and tray	220–260	150–170
Hot gas recycle	Pilot scale	Single catalyst bed (Cylindrical shell)	300–350	*
Oil recirculation	Pilot scale	Single catalyst bed (Cylindrical shell)	220–270	*
Fixed fluidized bed	Commercial	Cylindrical shell Heat transfer through tube bundle in bed	300–330	450
Slurry phase	Commercial	Cylindrical shell Heat transfer through tube bundle in bed	200–320	200

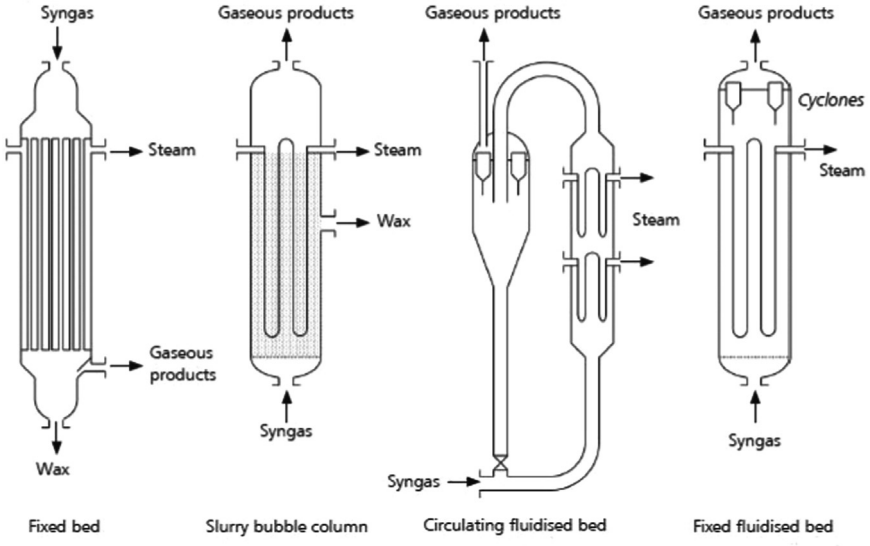

Fig. 11. Commercial FT reactors [176].

The second type of commercial LTFT reactor is the slurry phase bubble column reactors where catalyst powders with dimensions of 10–200 μm are used. As a result, the effect of internal mass transfer resistances is negligible resulting in optimal activity and selectivity. Also, the efficient heat removal system allows nearly isothermal operation of the catalytic bed. Productivity in a slurry bubble column reactor is higher than in a fixed bed reactor due to increased catalyst utilization and greater average reactor temperature. Difficulty in scale up of slurry bubble column reactors and solid catalyst separation posed issues towards the commercialization of slurry bubble columns for FT process [113].

3.3.2. *High temperature FT reactor-HTFT*

High temperature FT processes operate in the temperature range of 300–350 °C utilizing Fe catalysts and producing gasoline or linear olefins [116,117]. The high temperatures vaporize all the products under reaction conditions, maintaining just two phases throughout the process [117]. These are called 2-phase fluidized bed systems. Two types of high temperature fluidized bed systems are in commercial use – fixed fluidized bed reactors and circulating fluidized bed (CFB) reactors. Fixed fluidized bed reactors are also called Sasol Advanced Synthol (SAS) reactors [112]. The high temperature FT technology exercised by Sasol in the Synthol process, South Africa, is the largest commercial scale application of the FT process [118]. SAS reactors that were successfully used for 30 years at Sasol are more economic compared to the CFB – primarily due to lesser structural complexity (like the suspended reactor–hopper–standpipe system of CFB). Duvenhage and Shingles [119] list major advantages of SAS over CFB as higher pass per conversion; lower catalyst consumption; uniform product selectivity with products in the range of slightly heavier hydrocarbons; less maintenance and easier construction. Cyclone separators of SAS very effectively retain the catalyst within the reactor. However, in case of CFB reactors, scrubber towers need to be used downstream of the cyclones to remove the last traces of catalyst before the product stream can be condensed [120].

3.3.3. *Micro and monolithic FT reactors*

Advanced reactor technologies are being investigated to improve the reaction rates and heat and mass transfer characteristics that are commonly observed as issues in commercially established reactors. Micro-structured reactors have been proposed and are

being developed for FT processes. These reactors include two sets of small parallel channels with one used for FT reaction and the other for circulating cooling water, thus increasing the efficiency of heat transfer between channels and resulting in isothermal operation [121]. Other advantages include high gas–liquid mass transfer rates in two-phase flow, high liquid and gas throughputs, low pressure drop and no wax-catalyst separation necessary [122]. Industries presently working to develop micro-structured based FT reactors are *Oxford Catalyst Group PLC* and *Compact GTL*. Technical complexity, cost, and catalyst inventory required are some of the major challenges [121].

Monolithic catalysts are ceramic structures made of cordierite or catalyst supports like alumina or silica, as shown in Fig. 12. The channel diameter range one to few millimetres with wall thickness ~ 0.1–0.3 mm. Above all, compared to fixed bed reactors, the diffusion distance is an order of magnitude smaller for monolithic catalysts. Most common method of depositing active metal on the monolith support is by washcoating. For monolithic catalysts, heat transfer in the radial direction is slow, calling for the need of an external heat exchanger for removal of heat of reaction, as shown in Fig. 13. Heavy liquid products can be recycled to the monolithic reactor and external heat exchanger is used to transport heat [123].

Ability to apply thin catalyst layers with a varying thickness over monolith materials eliminates the effects of diffusion limitations and allows designing of monolithic catalysts with optimal activity and selectivity. Catalyst layers of magnitude less than 50 μm are free of diffusion limitations, showing highest activity and selectivity to C_{5+} products. However, monoliths with thicker washcoats experience internal diffusion limitations [124]. Monolithic catalysts could serve an interesting alternative to conventional catalysts for FT synthesis, the crucial problem being, its fragility and imperfect channel structure [125].

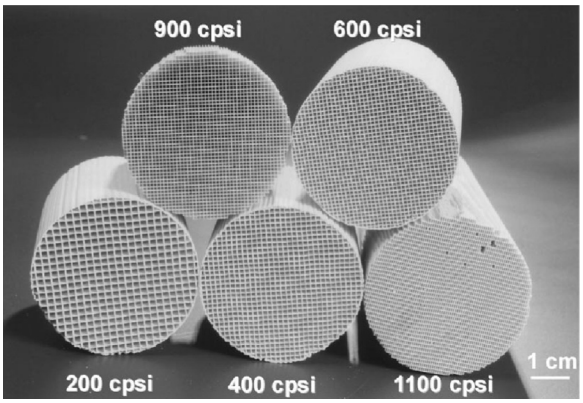

Fig. 12. Monolith structures [123].

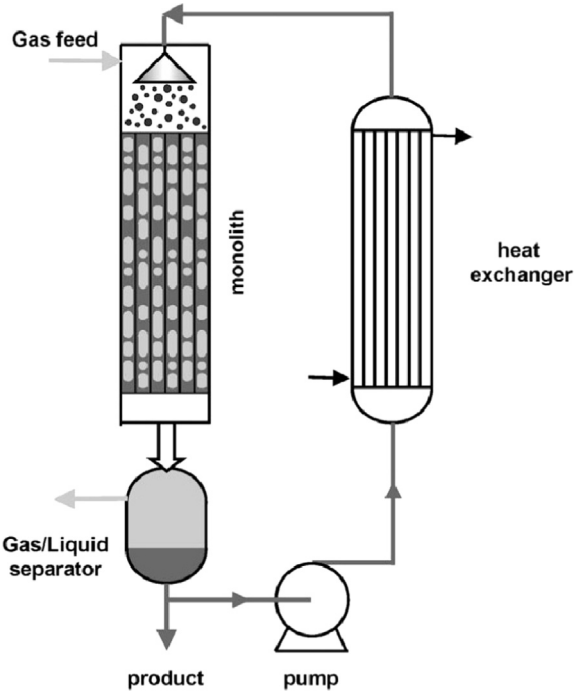

Fig. 13. Monolithic loop reactor with liquid recycle [123].

4. FT products

FT reaction produces a wide range of hydrocarbon and oxygenated hydrocarbon products. Selectivity of CH_4, an unwanted product, can vary from as low as 1–100%. At the other end of this product spectrum, the selectivity of long chain linear waxes can vary from zero to 70% with the intermediate carbon products produced only in limited amounts. The spread in C number can be varied by changing the operating temperature, the type of catalyst, the amount or type of promoter present, the feed gas composition, the operating pressure, or the type of reactor used [63]. FT synthesis should result in high selectivity towards desired products. C_{5+} paraffins, low- and intermediate-molecular-weight olefins, and C_{20+} linear hydrocarbons lead to the production of fuels and petrochemicals. Obviously, the selectivity of these products should be maximized. FT selectivity is governed by the polymerization type kinetics, dictating the chain growth processes during the catalytic reaction [126].

FT product distribution obtained from various catalysts show specific characteristics on cobalt, iron and ruthenium catalysts. Carbon-number distributions for FT products indicate the highest concentration for C_1 and decrease steadily for higher carbon numbers, though around C_3–C_4 often a local maximum is observed, as shown in Fig. 14. Monomethyl-substituted hydrocarbons exist in mild amounts, and dimethyl products occur in significantly smaller amounts than mono-methyl. Strikingly, none of the branched products contain quaternary carbon atoms. A variation in chain growth parameter in the distribution is observed only for linear paraffins, not for olefins. Alcohol yields are maximal at C_2 and decrease with carbon number [127].

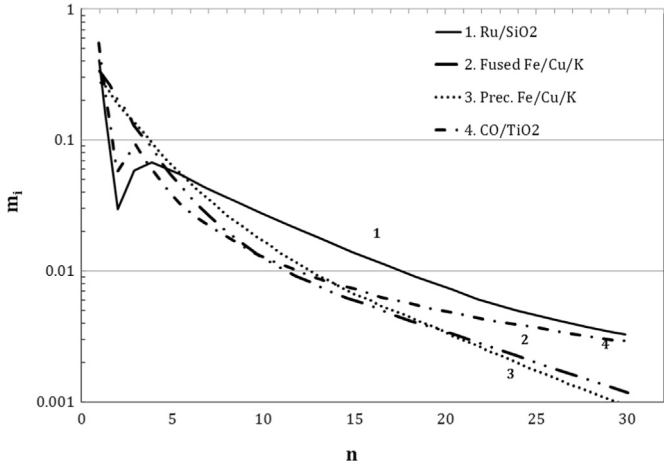

Fig. 14. Total hydrocarbon selectivity on Co/TiO_2 (T=473 K, H_2/CO=2.1, P=2.0 MPa), Ru/SiO_2 (T=485 K, H_2/CO=2, P=0.51 MPa) and fused and precipitated Fe/Cu/K [127].

4.1. FT product distribution model

The spectrum of products formed during the FT process proposes a strong kinetic basis, provided the main surface reactions, and their conjunctions are well understood and based on carefully measured experimental data [128]. Several mechanisms have been put forth by many researchers for chain growth in FT synthesis. Herington reported stepwise addition model of single-carbon units which could anticipate the fraction of products at each carbon number [129]. His research assumed that n-paraffins and α- and β-olefins were generated by stepwise incorporation of a methylene radical to a growing chain on the surface of the catalyst. β_n, the probability of each carbon (C) number to occur as a product rather than grow to form longer chain hydrocarbons, is given by Eq. (8). Here m_n, is the mole fraction of carbon number n. Also, the experiments showed that β_n values stayed somewhat constant at 0.28 for olefins and paraffins from C_5 to C_{11}, formed on a cobalt catalyst. Herington also indicated that CH_4 mechanism resulted due to an alternate mechanism [130].

$$\beta_n = m_n / \sum_{n+1}^{\infty} m_i \tag{8}$$

Satterfield and Huff [130] suggested a method based on probability considerations. They predicted that methyl-substituted isomer distributions for saturated hydrocarbons, within any one C number ranging from C_5 to C_8, formed over the surface of the cobalt catalyst can be interrelated. In this study it was assumed that the build up of carbon skeleton is by addition of monomer unit to any terminal carbon atom (with a constant probability value, a) or any penultimate carbon atom (with a probability b). a and b values were deduced from experimental data. The assumed isomer concentrations in individual molecular-weight fractions matched with the experimental concentrations. An average deviation of 0.7% was recorded from the experimental values [131]. Assuming CH_2 as the monomer of the FT reaction, a CH_2 unit can react with H_2 to yield CH_4, which will then desorb from the surface, or the CH_2 monomer can link up with another CH_2 unit to form an adsorbed C_2H_4 species. Again, the C_2H_4 unit now has three options – it could desorb to yield ethene, or be hydrogenated to generate ethane, or it can join with another CH_2 monomer to generate an adsorbed C_3H_6 unit. The initial two actions are chain termination actions, and their combined possibility of occurring can be considered as the probability of chain termination. The third action is the probability of chain growth, α. These reaction sequences could progress resulting in production in hydrocarbons ranging from CH_4 to high molecular mass waxes. A higher value of α indicates the formation of longer hydrocarbon chains. Under steady state conditions, the concentration of each C_nH_{2n} species on the catalyst surface should be constant. If α is the chain growth probability, then $(1-\alpha)$ is the probability of chain termination [63]. Fig. 15 shows hydrocarbon selectivity as a function of chain growth probability factor.

4.2. Factors affecting α

Within certain limits, α can be selected by adjusting FT process conditions like reaction temperature, H_2/CO ratio and catalyst composition. Low temperatures result in an FT products with a higher average carbon number, i.e. longer chain hydrocarbons (high α), with α ranging from 0.92 to 0.95 [79]. On the other hand at high temperatures, as in HTFT process, α value decreases [132]. At temperatures between 300 and 350 °C α values range from 0.65 to 0.70 [79]. Fig. 16 shows the variation of α as a function of temperature.

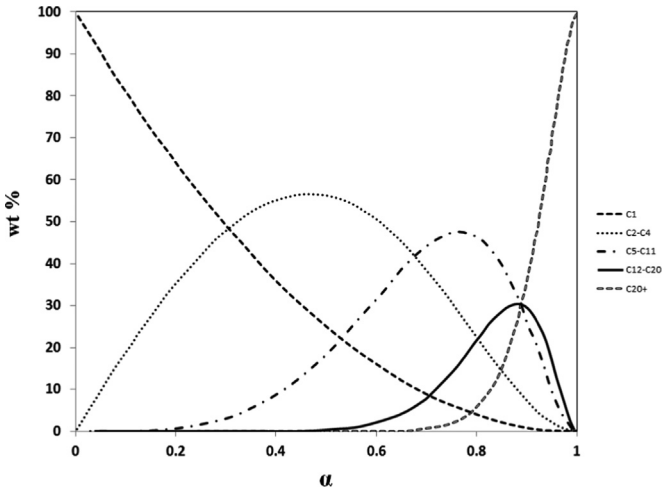

Fig. 15. Hydrocarbon selectivity as a function of the chain growth probability factor α [177].

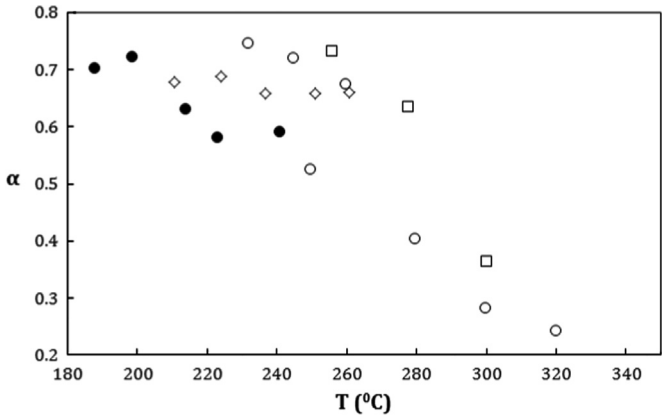

Fig. 16. Chain growth probability factor as a function of temperature. ○: Fe/Cu/K commercial Ruhrchemie catalyst, gas-slurry system, $(H_2/CO)_{feed}$=0.7, 2.72 MPa, $0.33*10^{-4}Nm^3kg^{-1}s^{-1}$; ●: Fe_2O_3 catalyst, gas solid system, $(H_2/CO)_{feed}$=3, 0.8 MPa; ◇:Fe_2O_3/K catalyst, gas solid system, $(H_2/CO)_{feed}$=3, 0.8 MPa; □:Ru catalyst, gas solid system, $(H_2/CO)_{feed}$=3, 0.8 MPa [127].

Reduction of H_2/CO feed ratio results in an FT product spectrum with higher average C number. Rise in H_2/CO partial pressure results in increased concentration of surface H_2, thereby raising the rate of H_2 termination steps relative to propagation and hence reducing chain growth probability [133]. In the case of cobalt catalysts, an increase in CO partial pressure increases α (from 0.86 at H_2/CO=3 to 0.90 at H_2/CO=1 at T=230 °C) and decreases CH_4 selectivity (from 16.4% at H_2/CO=3 to 4.2% at H_2/CO=1, T=230 °C). At low CO concentrations, CH_4 selectivity is high. Therefore, these conditions need to be prevented in an FT reactor when cobalt based catalysts are used [60]. Fig. 17 shows the variation of chain growth probability factor with varying H_2/CO ratio.

Catalyst composition also affects the chain growth. Electronic effect of potassium promoter enhances the electron-donor effect of the Fe catalyst, thereby facilitating CO adsorption and the dissociation of the C–O bond while reducing the metal-hydrogen and metal-oxygen bond strength. Due to this the carbon consumption reactions including the chain growth reactions are intensified [79]. However, a minimal effect of promoters is observed on the activity and selectivity of cobalt catalysts. Rhenium increases the rate of reduction of cobalt oxide to metallic cobalt and also improves the selectivity to long chain hydrocarbons [134]. Escalona et al. [135] analysed the effect of the addition of Cu, Zn, Re and Ru at two varied compositions on Co/SiO_2 catalysts. They reported that both

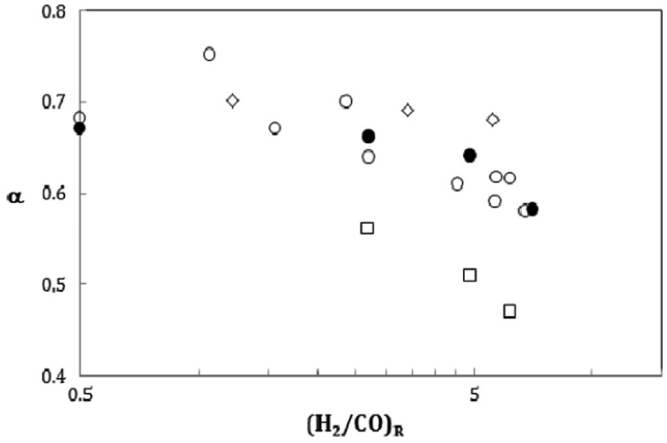

Fig. 17. Chain growth probability factor as a function of H_2/CO ratio. ○: Fe/Cu/K catalyst, gas slurry system, 1.48 MPa, 260 °C; ●: Fe_2O_3 catalyst, gas solid system, 212 °C, 0.5–1.2 MPa; ◇: Fe_2O_3/K catalyst, gas solid system, 240 °C, 0.8 MPa; □: Ru catalyst, gas solid system, 275 °C, 0.8 MPa; ⊙: Fe/Cu/K commercial Ruhrchemie catalyst, gas solid system, 250 °C, 1.0–2.5 MPa [127].

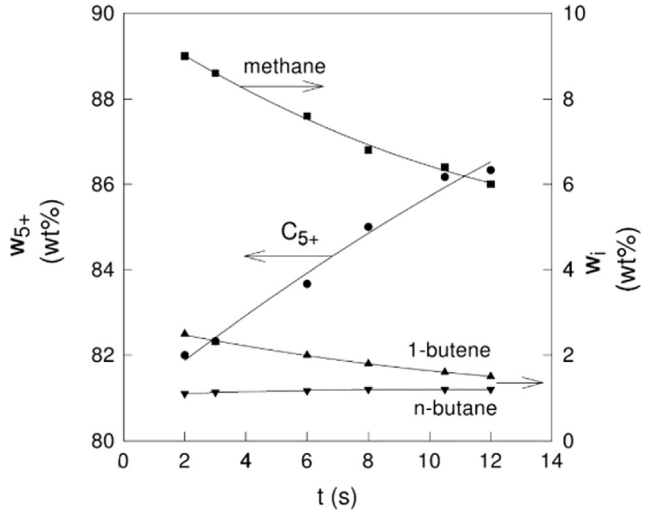

Fig. 18. Residence time effect on methane, C_{5+}, n-butane, and 1-butene selectivity on Co/TiO_2 (473 K, 2.0 MPa, H_2CO=2.1, 9.5–7.2% CO conversion [127].

reducibility and dispersion of cobalt species are affected by the addition of promoters.

On increasing the space velocity the products from FT synthesis utilize reduced time on the catalyst surface and hence the probability of re-adsorption and reaction becomes less, thereby reducing the extent of secondary reactions. Increasing the space velocity reduces conversion resulting in higher CO partial pressure at the reactor outlet, which additionally lowers secondary reactions [66]. Fig. 18 shows the effect of residence time on methane, C_{5+}, n-butane, and 1-butene selectivity on Co/TiO_2 catalyst. The methane and olefins selectivity reduces with decreasing space velocity while the paraffin selectivity remains unaffected [127].

Table 5 summarizes the overall influence of FT operating conditions on product selectivity. Table 6 lists the operating α of commercial FT plants. Based on the data in Table 6 and Fig. 19, commercial FT plants operate with α in one of the two regimes – 0.82–0.85 or 0.90–0.95. Choice of α is exclusively dependent on the product spectrum desired from the FT plant. Considering the FT kinetics, maximum yield of C10–C20 hydrocarbons is 40% at α=0.85. For higher yields of these hydrocarbons the FT reactor must be designed in such a way that the operating α is above 0.90,

Table 5
Influence of FT operating conditions on product selectivity [66].

Selectivity parameter	Operating parameter being increased			
	Temperature	Pressure	Space velocity	H_2:CO ratio
Carbon number distribution	Lower α-value	Higher α-value	No change[a]	Lower α-value
Methane selectivity	Increases	Decreases	Decreases	Increases
Alkene selectivity	–[b]	–[b]	Increases	Decreases
Oxygenate selectivity	–[b]	Increases	Increases	Decreases
Aromatic selectivity	Increases	–[b]	Decreases	Decreases
Syngas conversion	Increases	Increases	Decreases	–[b]

[a] Change is possible if secondary reactions are significant.
[b] The direction of change depends on a more complex relationship.

Table 6
α for commercially operating FT plants.

Plant	Reactor	Catalyst	α[a]
American Hydrocol facility	Fixed fluidized bed T=305–340 °C P=27 bar	Fused Fe	**<0.7**
Sasol 1 - Kellogg Synthol Process	Circulating fluidized bed (CFB) T=290–340 °C P=22 bar	Fused Fe	**<0.7**
Arge LTFT synthesis	Multi-tubular fixed bed T=200–250 °C P=25–27 bar	Precipitated Fe	**0.90**
Sasol slurry bed process (SSBP)	Slurry bed *(catalyst suspended in liquid wax)* T=245 °C P=21 bar	Precipitated Fe	**0.95**
Sasol Advanced Synthol (SAS)	Fixed fluidized bed T=310–350 °C P=25 bar	Fused Fe	**0.7–0.8**
Mossgass facility	Sasol Synthol CFB T=330–360 °C P=25 bar	Fused Fe	**0.7–0.8**
Shell middle distillate synthesis (SMDS)	Multi-tubular fixed bed T=220 °C P=25 bar	Co based	**0.90–0.92**
Oryx-GTL facility	Sasol slurry phase distillate T=230 °C P=20–25 bar	Co/Pt/Al_2O_3	**0.90–0.92**

[a] α values derived from [42,178–180].

so that the wax compounds can be hydro-cracked to hydrocarbons in the C_{10}–C_{20} range [42].

5. Biomass based FT fuels

5.1. Environmental impacts of BTL

The underlying idea for utilizing biomass as a renewable energy resource dwells in trapping the incoming solar energy and carbon from the atmospheric CO_2 in growing biomass. This

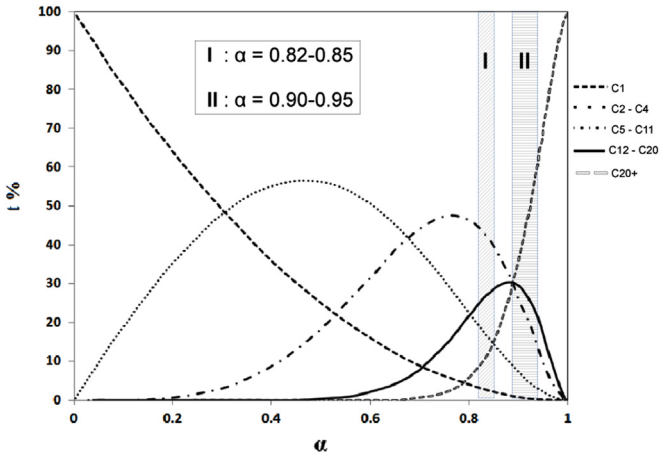

Fig. 19. ASF plot with the α regimes for commercially operating FT plants.

biomass is then converted to other fuels (biofuels, synfuels, hydrogen), used directly as a source of thermal energy, or is treated to be converted to other chemicals [136]. As a consequence, the prodigious advantage of employing biomass as a feedstock for producing synthetic fuel is that no CO_2 sequestration is necessary and most importantly, for CO_2 sequestration process followed by BTL, the result is carbon negative [137]. Clearing carbon rich habitats for biofuel production would increase CO_2 emissions in copious amounts relative to emissions released by use of fossil fuels. Hence, generation of biofuels from perennials grown on degraded crop lands and from waste biomass can reduce habitat destruction, competition with food production, and thereupon carbon debts [138,139]. Fleming et al. [140] evaluated a 91% lower well-to-wheel GHG emissions for lignocellulosic derived FT liquids, as compared to the reference gasoline baseline. Jungbluth et al. [141] reported that a 60% reduction in the transport sector related GHG emissions can be achieved with the use of FT-BTL processes. However, this reduction can only be achieved if short rotation wood or straw is used as the biomass input instead of agricultural biomass. The production of BTL fuels from energy crops results in emission of matter that contribute to the eutrophication and acidification. These emissions are greater than those of fossil based fuels used in the transportation sector. Therefore, the GHG emissions significantly depend on the biomass feedstock choice. Biofuels derived from industrial waste and residues are likely to result in maximum GHG reductions. Above all, these sources prevent the socio-environmental impacts such as competing for food crops, soil nutrient restoration, eutrophication and acidification that otherwise commonly result due to the steady production of crop or timber-wood for BTL applications. Haase et al. [142] showed emissions from FT fuels obtained from short rotation wood leading to higher acidification compared to FT fuels derived from residual forest wood.

From a detailed well to wheel analysis, it has been estimated that the FT diesel vehicles utilize 1.3–2.9 MJ of additional energy per kilometre compared to a fossil fuel derived diesel. The higher total energy use for diesel is due to a comparatively low conversion efficiency of BTL system. Nevertheless, a majority of this energy is obtained from renewable sources, yielding fossil energy savings of 0.9–2.1 MJ/km [5]. Table 7 gives the GHG emissions per kilometre with respect to gCO_2-eq./km for various sources of transportation fuels. Use of fossil fuel derived gasoline produces maximum GHG emissions with 210–220 gCO_2-eq./km. Contrastingly, FT fuels derived from biomass yields lowest GHG emissions, ranging from 15 to 115 gCO_2-eq./km. Such a wide range of variation in the GHG emissions from BTL fuel is due to the difference in the CO_2 sequestration rates of individual sources of biomass. FT

Table 7
GHG emissions for various fuels.

Fuel	Source	GHG emissions (gCO_2-eq./km)
FT-Diesel	Waste wood	15
FT-Diesel	Short rotation forestry	80–120
Bio-ethanol	Sugarcane	50–75
Bio-ethanol	Corn, sugarbeet, wheat	100–195
Biogas	Fermentable wastes	25–100
Biodiesel	Rapeseed, jatropha, sunflower	80–100
Gasoline	Fossil	210–220
Diesel	Fossil	185–220
Natural gas	Fossil	155–185

diesel produced by CTL process increases CO_2 emission rather than reducing them. Use of advanced technologies like carbon capture and storage (CCS) in CTL plants would not reduce the GHG emissions as much as the BTL process tends to reduce [38]. Recent studies have revealed the ability of CO_2 hydrogenation over FT catalyst for varying $H_2/CO/CO_2$ mixtures [143–145]. CO_2 from CCS units can be used as an active fuel in the FT reactor for conversion to liquid transportation fuel. H_2 for the FT reactor can also be obtained from renewable sources other than biomass gasification, such as photocatalytic splitting of water, catalytic processing of alcohols and bio-fuels [146–150]. These alternative sources of H_2 along with innovative CO_2 capture technologies [151–155,146] could be coupled to any FT reactor to obtain liquid fuels.

The quality of diesel produced by FT process is very high, with cetane number up to 75 [156]. FT products are devoid of sulphur, nitrogen, nickel, vanadium, asphaltenes, and aromatics that are observed in products obtained from mineral oil [157]. Naphtha generated by FT process has a lower octane number than conventionally derived naphtha. Also, FT-liquids are conceivably well suited for use in fuel cell vehicles (FCVs), which need clean fuel to avoid contamination of fuel cell catalyst [158]. Simultaneously, the rise in demand of diesel and a marginal increase in production of fossil diesel fuels would keep the oil prices high [38].

5.2. BTL economy

The syngas conversion efficiencies have a direct impact on the overall BTL economics. Besides efficient reactor design, the effectiveness of catalysts has a paramount influence on the production rates and hence on the cost of the generated liquid fuel. Gasification efficiencies, syngas conditioning energy demands, FT conversion rates and the FT crude upgrading efficiencies together dictate the economic viability of the BTL plant. In general, the oxy-steam biomass gasifier has a gasification efficiency in the range of 75–81% [56,159]. Further, the syngas to liquid fuel efficiency for a cobalt based FT reaction unit ranges from 35% to 50%, resulting in an overall biomass to liquid fuel efficiency in the range of 28–40%. Advanced performance catalysts and improved reactor design coupled with economically viable operations (catalyst bed residence time, reactor size, recycle ratio) can result in improved BTL efficiencies. The single pass hydrocarbon yield of catalysts, at CO conversions in the range of 40–50% and weight hourly space velocity of 2200–2500 $ml/h \cdot g_{cat}$, varies in the range of 0.1–0.3 $g\text{-}C_{5+}/g_{syngas}$. Under these conditions, the biomass to liquid fuel efficiencies range from 20% to 34%. The overall BTL efficiencies can be improved to 50–55% by synthesizing high yielding catalysts and designing efficient FT reactors with high heat transfer rates, along with improved technologies for O_2 generation, syngas purification and CO_2 separation, as required in the gasification process.

In single pass FT reactors, a considerable fraction of the FT products remains in the gas phase. Therefore, utilization of the unconverted syngas and gas phase hydrocarbons for in-house

thermal and electricity applications propitiously influence the FT economics. Additionally, the sale of generated electricity to the grid can further reduce the cost of liquid fuel generated in the BTL process. Larson et al. [159] showed a 50% decrease in the liquid fuel cost with a 75% increase in the price of electricity sale. The techno-economic analysis of an FT based BTL system using a 24 t/d oxy-steam biomass gasifier, coupled to a fixed bed, cobalt based FT reactor was evaluated by the Combustion and Gasification group at the Indian Institute of Science. The BTL unit was designed to produce liquid fuel at the rate of 40–45 b/d. For an Indian scenario, the diesel costs were estimated in the range of 0.6–0.8$/l. The calculated diesel prices were equivalent to the market diesel price and strongly evidenced a competitive and sustainable production of biomass derived FT fuels.

The cost of biomass is another major factor deciding the cost of BTL liquid fuel. Anticipating biomass cost is challenging since it is coupled with several factors, such as local supply chain, resource availability, processing costs, land availability, deforestation risks, simultaneous competitive uses and the sustainability touchstone. Above all, the practicability of biomass based power plants is associated with the long term availability of biomass feedstock and low costs. Hence, a steady source of biomass at a reasonable cost is crucial for the sustainable operation of the FT plant. Locally obtained biomass such as industrial wastes, agricultural residues and municipal solid wastes can be ideally processed as a fuel for syngas production and subsequent conversion to liquid fuels [160].

The economy of the BTL fuel production is an important parameter that dictates the optimum scale of each BTL project. Since fuel synthesis is coupled with steep investment costs, large-scale production is essential to obtain effective returns. However, small-scale plants could utilize cheap local biomass for reduced transport costs and directly take care of higher investment costs [161]. Table 8 compares the techno-economic aspects of BTL plants. In the process of production of liquid fuels (which can at once replace petroleum fuels), when the co-product electricity is sold at a reasonably high price, and/or the cost of biomass purchase is low, the cost of production of these liquid fuels could compete with petroleum products when oil prices are lower than $60/bbl [159]. The choice and usage of energy intensive processes in the BTL plant, which include air separation units, steam generator, CO_2 separator and gas compressors, invariably affect the liquid fuel cost. Economic development due to bigger production scales, advances in gasification technology and increased efficiencies through improved catalysts is most likely to increase the competitiveness of biofuels in the energy market [162].

5.3. BTL installations

At present, there are a few BTL plants on a commercial scale. These are still small compared to the coal or natural gas based FT plants as established by SASOL in South Africa or by SHELL in Malaysia. Gas cleaning between reactors poses a primary issue when biomass gasification is integrated with FT synthesis. Apart from CO and H_2, the gas generated contains a number of contaminants which need to be removed before reaching the FT unit, which is extremely susceptible to impurities like tar, BTX (benzene, toluene, and xylenes), inorganic impurities (NH_3, HCN, H_2S, COS, and HCl) and volatile metals, dust and soot. These impurities can be reduced by proper choice of gasification conditions and reactor design [163–166]. It is very essential to clean the syngas carefully before entering into the FT reactor. The cost of cleaning and regeneration of FT catalysts must be evaluated carefully also to account for the loss in production due to the poisoning of the catalyst [164]. BTL systems consist of many processes, hence stable and steady operation of the integrated system is critical.

Table 9 lists the established BTL plants. The CHOREN plant which is the world's only large scale commercial BTL plant utilizes a high temperature Carbo V gasifier to produce syngas with composition (vol%), H_2=64.5, CO=31.9, CO_2=2.5, N_2=0.8, CH_4=0.1 and H_2O=0.2. This plant utilizes 3000 t/d of dry woody biomass to produce 5000 b/d of FT oil [167,168]. Velocys, with their proprietary combustion synthesized cobalt catalysts and microchannel reactors, have commercialized the BTL process, producing liquid fuels in the range of 2000–1500 b/d [169]. These plants, as indicated in Table 9, generate liquid fuels from a wide range of biomass sources that include, municipal and commercial waste, forest and saw-mill waste, forest and agricultural residue and dry woody biomass. The gasification capacities of these plants vary from 500 t/d to 150 t/d of dry biomass. Recent interests of the aviation industries in the production and use of environment friendly jet fuels have resulted in the large scale development of BTL projects [170]. *British Airways, Cathay Pacific Airways and Southwest Airlines* have started developmental projects that use wastes to produce bio-jet fuels using gasification and FT synthesis. The GreenSky project, Fulkrum Bioenergy and Red Rock biofuels, indicated in Table 9, are being constructed to produce jet fuels from biomass resources. Long term operation of bench-scale BTL systems was examined by Kim et al. [171]. The test setup consisted of bubbling fluidized bed (BFB) gasifier (20 kW_{th}), gas cleaning unit, syngas compression unit, acid gas removing unit and an FT reactor. The integrated unit was run for a total time of 500 h. Overall C_{5+} selectivity was above 50% with output of 0.1 b/d [171].

A principal factor to be considered for the establishment of large scale BTL plant is the availability of biomass, which is a limiting factor for the scale up of biomass gasification unit. If a choice has to be made for the construction of large scale FT plants, options for converting agricultural residue and waste to syngas have to considered, along with remotely obtained syngas. Resources such as municipal solid wastes (MSW), agricultural residues and plantation residues can be converted to liquid

Table 8
Techno-economic review for FT based BTL.

Fuel	Process	Production capacity (bpd)	Liquid fuel cost ($/l)
Switch grass [159]	• Pressurized O_2 blown fluidized bed gasifier • 4545 t/d feed	4630	0.52 • Slurry bed FT reactor
Residual wood straw [181]	• Pressurized O_2 blown entrained flow gasifier • 5000 t/d feed	5500	1.57 • Fixed bed FT reactor
Corn stover [182]	• Pressurized oxy-steam fluidized bed gasifier • 2000 t/d feed	2362	1.39 • Fixed bed FT reactor
Woody biomass [161]	• Pressurized O_2 blown fluidized bed gasifier • 1000 t/d feed	1700	0.81 • Slurry bed FT reactor
Woody biomass [162]	• Entrained flow gasifier • 2000 t/d feed	2180	0.4 • Fluidized bed FT reactor

Table 9
BTL installations.

Organization	Year	Gasifier	Scale	Details
Solena Fuels, *Green Sky* (Essex, UK)	2015	Solena plasma gasification	Commercial • 1157 bpd jet fuel • Co catalyst • Velocys micro-channel reactor	• Municipal & commercial waste
Red Rock Biofuels (Oregon, USA)	2017	TRI steam reformer	Commercial • 460 t/d biomass feed • 1100 bpd liquid fuel • Co catalyst • Velocys reactor	• Forest & saw mill waste
Sierra Biofuels, *Fulkrum Bio-energy* (Nevada, USA)	2016	TRI steam reformer	Commercial • 400 t/d MSW feed • 657 bpd liquid fuel • Co catalyst • Velocys reactor	• Municipal solid waste
SYNDIESE, *CEA* (Nevada, USA)	2015	Entrained flow, O_2 blown, high pressure gasifier	Commercial	• Forest & agricultural waste • 205 t/d biomass feed • 530 bpd liquid fuel
CHOREN, [183,184] Sigma Plant (Freiberg, Germany)	2010	*Carbo-V* gasification	Commercial • 5000 bpd liquid fuel • Co catalyst • Fixed bed reactor • *temporarily discontinued*	• 3044 t/d dry biomass
Velocys [185] (Gussing, Austria)	2010	Dual Fluidized bed gasifier	Pilot • 1 bpd FT products • Micro channel reactor • Co catalyst	• 150 t/d dry biomass
CUTEC [185] (Germany)	2010	CFB, steam-O_2 gasification	Laboratory • Fixed bed, Co catalyst • 2500 hours of gasifier operation • 900 hours of FT operation • 150 ml/day FT products	• 2.7 t/d dry biomass

hydrocarbons effectively, economically and with favourable environmental returns if wide range of input feed and output products are handled using a beneficial technique. In most cases, MSW can be gasified to generate syngas for BTL application. The technologies for converting waste to electricity or liquid fuels and chemicals were described by Hossain et al. [172]. A troubling fact with the utilization of MSW for BTL implementation is the wide class of solid wastes and their compositions which vary with time as well as location. Notably, strict policies to separate organic wastes from the inorganic components (*compounds of lead, mercury, iron, copper*) need to be implemented actively for realizing waste to energy projects [22]. Organic residues from waste water sludge can also be separated and treated for generating syngas by gasification and subsequent production of liquid fuels via FT synthesis. The process of converting sludge to biofuel stage is still in developmental stage and, the mechanical de-watering and drying pose an extensive challenge for commercializing this process [173].

Such conversions can be achieved in a bio-refinery that can handle this wide range of feedstock and output products including special chemicals. Most importantly, if the tail gas from FT reactor is not recycled, again, the residual gases can be converted to electricity, which serves as a propitious co-product from the FT reactor.

6. Concluding observations

This paper consolidates the research and developmental efforts that have taken place in the area of FT process. Conversion of biomass derived syngas to liquid transportation fuel via FT synthesis is a promising technique and attaining importance in recent years – to meet the ever-increasing energy demands and conform to stricter environmental regulations. The paramount benefit of synthesizing liquid hydrocarbon fuel from biomass via FT process is the fact that the FT technology is fairly advanced. Therefore, large scale installations of FT synthesis plants can be attained without any great technical barriers. As discussed earlier, the bio-energy systems usually demand non-renewable energy, used for its production, processing, transportation, and subsequent transformation to bio-fuels. Fossil fuel derived gasoline, diesel and natural gas have the energy ratio (*ratio of the energy output of the end product to the fossil energy required for producing the desired fuel*) ranging from 0.83 to 0.95. Comparatively, the bio-diesel derived from waste vegetables by transesterification have the energy ratio of 5–6, the palm oil derived transesterified bio-diesel have energy ratio in the range of 8.5–9.5 and, the liquid fuels derived from bio-syngas, via FT process, yield an energy ratio in the range of 3–6.8. Palm oil, derived by the transesterification process, has resulted in high oil productivity compared to other oil seeds. The average yield of palm oil can be increased from 3.7 t/ha/year to over 10 t/ha/year by using high quality seeds. However, such plants require tropical climate conditions that include heavy rainfall (1500–2000 mm, without long drought durations), temperatures ranging from 25 to 30 °C, humidity greater than 75% and, at least 1500 h of annual sunshine. To obtain sustainable yield of oil from land crops, the oil crop should be cultivated on waste land that are not part of the agricultural land [22]. Malaysian palm oil board is working to develop 60,000 tonnes per annum palm oil diesel plant and set a target to replace more than 5% of crude oil obtained diesel with palm oil diesel [174]. But, the striking advantage of the FT derived liquid fuels is that the liquid fuels

obtained from FT process have similar combustion properties as the gasoline and diesel obtained from petroleum sources. The calorific value of bio-diesel obtained from palm oil, via the trans-esterification process, has 10% lower heating value compared to neat diesel. Conclusively, the BTL liquid fuels obtained through FT reaction can be conveniently produced on large scale and can replace the fossil derived transportation fuel directly without altering the properties of the combustion devices or its efficiencies. Other processes for obtaining liquid transportation fuels from biomass sources like fast pyrolysis, transesterification of vegetable oils and bio-oil from algae suffer from major drawbacks such as low quality fuels, low energy efficiency and obstruction to large scale commercialization due to low energy ratios and lower economic returns. FT process, on the other hand, is a well-established process that can be coupled to a biomass gasification system.

In general, biomass derived syngas using air gasification process is deficient in H_2. The use of steam and oxygen as gasification units enhance the H_2 content in the syngas. The steam to biomass ratio can be adjusted to vary the H_2/CO ratio in the syngas for compatibility with the FT synthesis. Based on the nature of the desired FT product spectrum, a choice predominantly exists for the selection of cobalt or iron catalyst. The choice of reactors coupled with active, long-life catalysts are crucial for a sustainable performance of the BTL plant. The detailed annualized life cycle analysis of a BTL system indicates that the production of electricity as a co-product results in the production of liquid fuels that are competitive with the market prices. Recent developments in the synthesis of active cobalt catalysts, synthesized by novel combustion methods, have improved the syngas to liquid conversion efficiencies in the range of 35–40%. With the inclusion of exported electricity from the BTL plant, the overall biomass to liquid fuel efficiency using FT process can be expected to be in the range of 35–40%. Understanding of the functioning of FT catalysts, reaction mechanism and kinetics along with aspects related to FT process conditions and the products suggest the need for further work in BTL sector. From the spectrum of results conducted in this study, it is evident that to obtain products of liquid transportation fuel quality, the chain growth probability factor, α must be in the range of 0.82–0.85. Reactor design, process conditions and the catalysts used are the conditions that affect the production rate and product quality of desired hydrocarbon fraction required from FT reactor.

Another concern with the production of liquid fuels is related to the fluctuating oil prices since low oil price can unreasonably affect the large scale BTL processes. Invariably, development of small scale BTL plants, tuned to produce variable product spectrum, that include a wide range of chemicals can sustain the impact of varying oil prices. The continued availability of biomass at low costs is crucial for the extended and sustained functioning of the BTL plant. For this reason, it is imperative that locally available biomass is used that comprise forest wastes, agriculture residues, industrial wastes and municipal solid wastes, apart from energy plants that are cultivated exclusively for the generation of liquid fuels.

This paper concludes that economically affordable and environmentally favourable BTL systems present a positively clean carbon neutral transportation fuel that can be used directly in the existing transportation sector provided the biomass is sustainably grown, transported, converted and consumed. A techno-economic analysis is also made based on the available data in the literature. For several developing countries, such as India, biomass to liquid fuel production via Fischer Tropsch synthesis can be achieved relatively easier as compared to industrialized countries. This is due to the better-growing climates, lower labour costs and in some cases, even lower capital costs.

Acknowledgement

The authors thank the Ministry of New and Renewable Energy (MNRE) of Government of India for the support provided. The authors gratefully acknowledge the advice and instructive discussions by Professor H.S. Mukunda.

References

[1] Gerssen-Gondelach S, Saygin D, Wicke B, Patel MK, Faaij A. Competing uses of biomass: assessment and comparison of the performance of bio-based heat, power, fuels and materials. Renew Sustain Energy Rev 2014;40:964–98.
[2] Conti J, Holtberg P. International energy outlook 2011. Washington, DC: Department of Energy, US Energy Information Administration; 2011.
[3] Midilli A, Dincer I. Hydrogen as a renewable and sustainable solution in reducing global fossil fuel consumption. Int J Hydrog Energy 2008;33 (16):4209–22.
[4] Eriksson G, Kjellström B. Assessment of combined heat and power (chp) integrated with wood-based ethanol production. Appl Energy 2010;87 (12):3632–41.
[5] Sunde K, Brekke A, Solberg B. Environmental impacts and costs of woody biomass-to-liquid (btl) production and use-a review. For Policy Econ 2011;13 (8):591–602.
[6] Dhillon R, von Wuehlisch G. Mitigation of global warming through renewable biomass. Biomass Bioenergy 2013;48:75–89.
[7] Hamelinck C, Faaij A. Outlook for advanced biofuels. Energy Policy 2006;34 (17):3268–83.
[8] Butterman H, Castaldi M. CO_2 as a carbon neutral fuel source via enhanced biomass gasification. Environ Sci Technol 2009;43(23):9030–7.
[9] Guo M, Song W, Buhain J. Bioenergy and biofuels: history, status, and perspective. Renew Sustain Energy Rev 2015;42:712–25.
[10] Goyal H, Seal D, Saxena R. Bio-fuels from thermochemical conversion of renewable resources: a review. Renew Sustain Energy Rev 2008;12(2):504–17.
[11] Bridgwater A, Meier D, Radlein D. An overview of fast pyrolysis of biomass. Org Geochem 1999;30(12):1479–93.
[12] Bridgwater A. Review of fast pyrolysis of biomass and product upgrading. Biomass Bioenergy 2012;38:68–94.
[13] Scott DS, Majerski P, Piskorz J, Radlein D. A second look at fast pyrolysis of biomassthe rti process. J Anal Appl Pyrolysis 1999;51(1):23–37.
[14] Sharma A, Pareek V, Zhang D. Biomass pyrolysis—a review of modelling, process parameters and catalytic studies. Renew Sustain Energy Rev 2015;50:1081–96.
[15] Brown RC, Holmgren J. Fast pyrolysis and bio-oil upgrading. Gas 2009;13:25.
[16] Wright MM, Daugaard DE, Satrio JA, Brown RC. Techno-economic analysis of biomass fast pyrolysis to transportation fuels. Fuel 2010;89:S2.
[17] Behrendt F, Neubauer Y, Oevermann M, Wilmes B, Zobel N. Direct liquefaction of biomass. Chem Eng Technol 2008;31(5):667–77.
[18] Bensaid S, Conti R, Fino D. Direct liquefaction of ligno-cellulosic residues for liquid fuel production. Fuel 2012;94:324–32.
[19] Toor SS, Rosendahl L, Rudolf A. Hydrothermal liquefaction of biomass: a review of subcritical water technologies. Energy 2011;36:2328–42.
[20] Shui H, Cai Z, Xu CC. Recent advances in direct coal liquefaction. Energies 2010;3(2):155–70.
[21] Robinson KK. Reaction engineering of direct coal liquefaction. Energies 2009;2(4):976–1006.
[22] Mukunda H. Understanding clean energy and fuels from biomass. India: Wiley; 2011.
[23] Pandey A, Press C. Handbook of plant-based biofuels. Boca Raton: CRC Press; 2009.
[24] Kim HJ, Kang BS, Kim MJ, Park YM, Kim DK, Lee JS, et al. Transesterification of vegetable oil to biodiesel using heterogeneous base catalyst. Catal Today 2004;93:315–20.
[25] Schuchardt U, Sercheli R, Vargas RM. Transesterification of vegetable oils: a review. J Braz Chem Soc 1998;9(3):199–210.
[26] Pradhan A, Shrestha D, McAloon A, Yee W, Haas M, Duffield J, et al. Energy life-cycle assessment of soybean biodiesel. United States, Department of Agriculture, Agricultural Economic Report 845; 200.
[27] Anselm E, Brown A, Fulton L. Technology roadmap: biofuels for transport. International Energy Agency; 2011.
[28] Chisti Y. Biodiesel from microalgae. Biotechnol Adv 2007;25(3):294–306.
[29] Gross M. Algal biofuel hopes. Current Biol 2008;18(2):R46–7.
[30] Demirbas MF. Biofuels from algae for sustainable development. Appl Energy 2011;88(10):3473–80.
[31] Kosinkova J, Doshi A, Maire J, Ristovski Z, Brown R, Rainey TJ. Measuring the regional availability of biomass for biofuels and the potential for microalgae. Renew Sustain Energy Rev 2015;49:1271–85.
[32] Achara N. Biofuel from algae. J Am Sci 2012;8(1):240–4.
[33] Chisti Y. Constraints to commercialization of algal fuels. J Biotechnol 2013;167(3):201–14.

[34] Liu X, Clarens AF, Colosi LM. Algae biodiesel has potential despite inconclusive results to date. Bioresour Technol 2012;104:803–6.
[35] Tijani H, Abdullah N, Yuzir A. Integration of microalgae biomass in biomethanation systems. Renew Sustain Energy Rev 2015;52:1610–22.
[36] Boerrigter H, den Uil H, Calis HP. Green diesel from biomass via Fischer–Tropsch synthesis: new insights in gas cleaning and process design, Pyrolysis and gasification of Biomass and waste, 2003, 1-13.
[37] van Steen E, Claeys M. Fischer–Tropsch catalysts for the biomass-to-liquid (btl)-process. Chem Eng Technol 2008;31(5):655–66.
[38] Van Vliet O, Faaij A, Turkenburg W. Fischer-tropsch diesel production in a well-to-wheel perspective: a carbon, energy flow and cost analysis. Energy Convers Manag 2009;50(4):855–76.
[39] Dupain X, Krul RA, Schaverien CJ, Makke M, Moulijn JA. Production of clean transportation fuels and lower olefins from Fischer–Tropsch synthesis waxes under fluid catalytic cracking conditions: the potential of highly paraffinic feedstocks for fcc. Appl Catal B: Environ 2006;63:277–95.
[40] de Klerk A. Hydroprocessing peculiarities of Fischer–Tropsch syncrude. Catal Today 2008;130:439–45.
[41] Fischer F. Brennstoff-chem 1923; 4:276; Fischer F, Tropsch H. Chem Ber B 1923;56:2428.
[42] Steynberg A. Introduction to Fischer–Tropsch technology. Stud Surf Sci Catal 2004;152:1–63.
[43] Schulz H. Short history and present trends of Fischer–Tropsch synthesis. Appl Catal A: Gen 1999;186(1):3–12.
[44] Dry M. The Fischer–Tropsch process: 1950–2000. Catal Today 2002;71(3):227–41.
[45] Wood DA, Nwaoha C, Towler BF. Gas-to-liquids (gtl): a review of an industry offering several routes for monetizing natural gas. J Nat Gas Sci Eng 2012;9:196–208.
[46] Dautzenberg K, Hanf J. Biofuel chain development in Germany: organisation, opportunities, and challenges. Energy Policy 2008;36(1):485–9.
[47] Gnanendra P, Ramesha D, Dasappa S. Preliminary investigation on the use of biogas sludge for gasification. Int J Sustain Energy 2012;31(4):251–67.
[48] Dasappa S, Sridhar H, Sridhar G, Paul P. Science and technology aspects of bio-residue gasification. Biomass Convers Biorefin 2011;1(3):121–31.
[49] Dasappa S, Subbukrishna D, Suresh K, Paul P, Prabhu G. Operational experience on a grid connected 100 kWe biomass gasification power plant in Karnataka, India. Energy Sustain Dev 2011;15(3):231–9.
[50] Dasappa S, Paul P, Mukunda H, Rajan N, Sridhar G, Sridhar H. Biomass gasification technology-a route to meet energy needs. Current Sci 2004;87(7):908–16.
[51] Dasappa S, Paul P, Mukunda H, Shrinivasa U. Wood-char gasification: experiments and analysis on single particles and packed beds. In: Symposium (International) on combustion, vol. 27. The Combustion Institute; 1998. p. 1335–42.
[52] Dasappa S. Potential of biomass energy for electricity generation in sub-Saharan Africa. Energy Sustain Dev 2011;15(3):203–13.
[53] Dasappa S, Sridhar G, Paul P. Adaptation of small capacity natural gas engine for producer gas operation. Proc Inst Mech Eng Part C: J Mech Eng Sci 2012;226(6):1568–78.
[54] Mukunda H, Dasappa S, Paul P, Rajan N, Shrinivasa U. Gasifiers and combustors for biomass-technology and field studies. Energy Sustain Dev 1994;1(3):27–38.
[55] Dasappa S, Sridhar G, Sridhar H, Rajan N, Paul P, Upasani A. Producer gas engines–proponent of clean energy technology. In: Proceedings of the 15th European biomass conference and exhibition; 2007. p. 976–80.
[56] Sandeep K, Dasappa S. Oxy-steam gasification of biomass for hydrogen rich syngas production using downdraft reactor configuration. Int J Energy Res 2014;38(2):174–88.
[57] Wilhelm D, Simbeck D, Karp A, Dickenson R. Syngas production for gas-to-liquids applications: technologies, issues and outlook. Fuel Process Technol 2001;71(1):139–48.
[58] Demirbas A. Progress and recent trends in biofuels. Progress Energy Combustion Sci 2007;33(1):1–18.
[59] Hassankiadeh MN, Khajehfard A, Golmohammadi M. Kinetic and product distribution modeling of Fischer–Tropsch synthesis in a fluidized bed reactor. Int J Chem Eng Appl 2012;3:400–3. http://dx.doi.org/10.7763/IJCEA.2012.V3.227.
[60] Subiranas A. Combining Fischer–Tropsch Synthesis (FTS) and hydrocarbon reactions in one reactor. Karlsruhe: Universitätsverl; 2009.
[61] Adesina AA. Hydrocarbon synthesis via Fischer–Tropsch reaction: travails and triumphs. Appl Catal A: Gen 1996;138(2):345–67.
[62] Pour AN, Housaindokht MR, Tayyari SF, Zarkesh J. Kinetics of the water-gas shift reaction in Fischer–Tropsch synthesis over a nano-structured iron catalyst. J Nat Gas Chem 2010;19(4):362–8.
[63] Dry M. Chemical concepts used for engineering purposes. Stud Surf Sci Catal 2004;152:196–257.
[64] Lögdberg S. Development of Fischer–Tropsch catalysis for gasified biomass [Ph.D. thesis]; 2007.
[65] Tavasoli A, Sadaghiani K, Nakhaeipour A, Ahangari M. Cobalt loading effects on the structure and activity for Fischer–Tropsch and water-gas shift reactions of Co/Al_2O_3 catalysts. Iran J Chem Chem Eng 2007;26(1).
[66] De Klerk A. Fischer–Tropsch refining. Wiley-VCH; 2011. p. 73–99 [chapter 4].
[67] Sarup B, Wojciechowski B. Studies of the Fischer–Tropsch synthesis on a cobalt catalyst ii. kinetics of carbon monoxide conversion to methane and to higher hydrocarbons. Can J Chem Eng 1989;67(1):62–74.
[68] van Steen E, Schulz H. Polymerisation kinetics of the Fischer–Tropsch Co hydrogenation using iron and cobalt based catalysts. Appl Catal A: Gen 1999;186(1):309–20.
[69] Overett M, Hill R, Moss J. Organometallic chemistry and surface science: mechanistic models for the Fischer–Tropsch synthesis. Coord Chem Rev 2000;206:581–605.
[70] Brady III R, Pettit R. Mechanism of the Fischer–Tropsch reaction. the chain propagation step. J Am Chem Soc 1981;103(5):1287–9.
[71] Wang CJ, Ekerdt JG. Evidence for alkyl intermediates during Fischer–Tropsch synthesis and their relation to hydrocarbon products. J Catal 1984;86:239–44.
[72] Schulz H, Beck K, Erich E. The Fischer–Tropsch co-hydrogenation. a non trivial surface polymerization selectivity of chain branching. In: Proceedings 9th international congress on catalysis: catalysis, theory to practice; vol. 2. Chemical Institute of Canada; 1988. p. 829.
[73] Johnston P, Joyner R. Structure-function relationships in heterogeneous catalysis: the embedded surface molecule approach and its applications. Stud Surf Sci Catal 1993;75:165–80.
[74] Maitlis PM. Fischer–Tropsch, organometallics, and other friends. J Organomet Chem 2004;689:4366–74.
[75] Turner M, Long H, Shenton A, Byers P, Maitlis P. The alkenyl mechanism for Fischer–Tropsch surface methylene polymerisation; the reactions of vinylic probes with Co/H_2 over rhodium catalyst. Chemistry—A European Journal 1995;1(8):549–56.
[76] Ndlovu S, Phala N, Hearshaw-Timme M, Beagly P, Moss J, Claeys M, et al. Some evidence refuting the alkenyl mechanism for chain growth in iron-based Fischer–Tropsch synthesis. Catal Today 2002;71(3):343–9.
[77] Davis B. Fischer–Tropsch synthesis: current mechanism and futuristic needs. Fuel Process Technol 2001;71(1):157–66.
[78] Huff Jr GA, Satterfield CN. Intrinsic kinetics of the Fischer–Tropsch synthesis on a reduced fused-magnetite catalyst. Ind Eng Chem Process Des Dev 1984;23(4):696–705.
[79] Claeys M, Van Steen E. Basic studies. Stud Surf Sci Catal 2004;152:601–80.
[80] Luque R, de la Osa A, Campelo J, Romero A, Valverde J, Sanchez P. Design and development of catalysts for Biomass-to-liquid-Fischer–Tropsch (btl-ft) processes for biofuels production. Energy Environ Sci 2012;5(1):5186–202.
[81] Li S, Krishnamoorthy S, Li A, Meitzner G, Iglesia E. Promoted iron-based catalysts for the Fischer–Tropsch synthesis: design, synthesis, site densities, and catalytic properties. J Catal 2002;206(2):202–17.
[82] Sie S, Krishna R. Fundamentals and selection of advanced Fischer–Tropsch reactors. Appl Catal A: Gen 1999;186(1):55–70.
[83] Dry M. FT catalysts. Stud Surf Sci Catal 2004;152:533–600.
[84] Zimmerman WH, Bukur DB. Reaction kinetics over iron catalysts used for the Fischer–Tropsch synthesis. Can J Chem Eng 1990;68(2):292–301.
[85] Ngantsoue-Hoc W, Zhang Y, OBrien RJ, Luo M, Davis BH. Fischer–Tropsch synthesis: activity and selectivity for group i alkali promoted iron-based catalysts. Appl Catal A: Gen 2002;236(1):77–89.
[86] Dictor RA, Bell AT. Fischer–Tropsch synthesis over reduced and unreduced iron oxide catalysts. J Catal 1986;97(1):121–36.
[87] Davis B. Fischer–Tropsch synthesis: relationship between iron catalyst composition and process variables. Catal Today 2003;84(1):83–98.
[88] Bukur DB, Koranne M, Lang X, Rao K, Huffman GP. Pretreatment effect studies with a precipitated iron Fischer–Tropsch catalyst. Appl Catal A: Gen 1995;126(1):85–113.
[89] Bukur D, Nowicki L, Manne R, Lang X. Activation studies with a precipitated iron catalyst for Fischer–Tropsch synthesis ii. Reaction studies. J Catal 1995;155(2):366–75.
[90] Bukur D, Mukesh D, Patel S. Promoter effects on precipitated iron catalysts for Fisher–Tropsch synthesis. Ind Eng Chem Res 1990;29(2):194–204.
[91] Jeon J, Kim C, Park Y, Ihm S. Catalytic properties of potassium- or lanthanum-promoted $Co/\gamma-Al_2O_3$ catalysts in carbon monoxide hydrogenation. Kor J Chem Eng 2004;21(2):365–9.
[92] Tao Z, Yang Y, Zhang C, Li T, Ding M, Xiang H, et al. Study of manganese promoter on a precipitated iron-based catalyst for Fischer–Tropsch synthesis. J Nat Gas Chem 2007;16(3):278–85.
[93] Schulz H, Riedel T, Schaub G. Fischer–Tropsch principles of co-hydrogenation on iron catalysts. Top Catal 2005;32(3–4):117–24.
[94] Soled S, Iglesia E, Fiato R. Activity and selectivity control in iron catalyzed Fischer–Tropsch synthesis. Catal Lett 1990;7(1–4):271–80.
[95] Rao Pendyala VR, Jacobs G, Mohandas JC, Luo M, Ma W, Gnanamani MK, et al. Fischer–Tropsch synthesis: attempt to tune fts and wgs by alkali promoting of iron catalysts. Appl Catal A: Gen 2010;389(1):131–9.
[96] Mokoena E. Synthesis and use of silica materials as supports for the Fischer–Tropsch reaction [Ph.D. thesis]; 2005.
[97] Iglesia E, Soled S, Fiato R, Via G. Bimetallic synergy in cobalt ruthenium Fischer–Tropsch synthesis catalysts. J Catal 1993;143(2):345–68.
[98] Yao Y, Liu X, Hildebrandt D, Glasser D. The effect of CO_2 on a cobalt-based catalyst for low temperature Fischer–Tropsch synthesis. Chem Eng J 2012:318–27.
[99] Iglesia E. Design, synthesis, and use of cobalt-based Fischer–Tropsch synthesis catalysts. Appl Catal A: Gen 1997;161(1):59–78.
[100] Snehesh S, Dasappa S. Characterization of SiO_2 supported co catalysts synthesized by solution combustion method for Fischer Tropsch synthesis. In: 8th international conference on environmental catalysis, Asheville, North Carolina, USA; 2014.

[101] Zavyalova U, Scholz P, Ondruschka B. Influence of cobalt precursor and fuels on the performance of combustion synthesized Co_3O_4/γ/-Al_2O_3 catalysts for total oxidation of methane. Appl Catal A Gen 2007;323:226–33.

[102] Toniolo J, Takimi A, Bergmann C. Nanostructured cobalt oxides (Co_3O_4 and CoO) and metallic Co powders synthesized by the solution combustion method. Mater Res Bull 2010;45(6):672–6.

[103] Shi L, Tao K, Kawabata T, Shimamura T, Zhang XJ, Tsubaki N. Surface impregnation combustion method to prepare nanostructured metallic catalysts without further reduction: as-burnt Co/SiO_2 catalysts for Fischer–Tropsch synthesis. ACS Catal 2011;1(10):1225–33.

[104] Jacobs G, Das TK, Zhang Y, Li J, Racoillet G, Davis BH. Fischer–Tropsch synthesis: support, loading, and promoter effects on the reducibility of cobalt catalysts. Appl Catal A: Gen 2002;233(1):263–81.

[105] Thiessen J, Rose A, Meyer J, Jess A, Curulla-Ferré D. Effects of manganese and reduction promoters on carbon nanotube supported cobalt catalysts in Fischer–Tropsch synthesis. Microporous Mesoporous Mater 2012;164:199–206.

[106] Davis BH. Fischer–Tropsch synthesis: comparison of performances of iron and cobalt catalysts. Ind Eng Chem Res 2007;46(26):8938–45.

[107] De Pontes M, Espinoza R, Nicolaides C, Scholtz J, Scurrell M. Natural gas conversion IV. Elsevier; 1997.

[108] Shi B, Davis BH. Fischer–Tropsch synthesis: the paraffin to olefin ratio as a function of carbon number. Catal Today 2005;106(1):129–31.

[109] Yates IC, Satterfield CN. Hydrocarbon selectivity from cobalt Fischer–Tropsch catalysts. Energy Fuels 1992;6(3):308–14.

[110] Yang Y, Xiang HW, Xu YY, Bai L, Li YW. Effect of potassium promoter on precipitated iron-manganese catalyst for Fischer–Tropsch synthesis. Appl Catal A: Gen 2004;266(2):181–94.

[111] Samiran B. Design and development of Fischer Tropsch reactor and catalysts and their interrelationships. Bull Catal Soc India 2007;6(1):1–22.

[112] Steynberg A, Dry M, Davis B, Breman B. Fischer–Tropsch reactors. Stud Surf Sci Catal 2004;152:64–195.

[113] Guettel R, Kunz U, Turek T. Reactors for Fischer–Tropsch synthesis. Chem Eng Technol 2008;31(5):746–54.

[114] Elbashir N, Bao B, El-Halwagi M. An approach to the design of advanced fischer-tropsch reactor for operation in near-critical and supercritical phase media. In: Advances in gas processing: proceedings of the 1st annual symposium on gas processing symposium; vol. 1; 2009. p. 423–33.

[115] Krishna R, Sie S. Design and scale-up of the Fischer–Tropsch bubble column slurry reactor. Fuel Process Technol 2000;64(1):73–105.

[116] Rahimpour M, Khademi M, Bahmanpour A. A comparison of conventional and optimized thermally coupled reactors for Fischer–Tropsch synthesis in gtl technology. Chem Eng Sci 2010;65(23):6206–14.

[117] Rahimpour M, Elekaei H. A comparative study of combination of Fischer–Tropsch synthesis reactors with hydrogen-permselective membrane in gtl technology. Fuel Process Technol 2009;90(6):747–61.

[118] Steynberg A, Espinoza R, Jager B, Vosloo A. High temperature Fischer–Tropsch synthesis in commercial practice. Appl Catal A: Gen 1999;186(1):41–54.

[119] Duvenhage DJ, Shingles T. Synthol reactor technology development. Catal Today 2002;71(3):301–5.

[120] Jager B. Development of fischer tropsch reactors. Prepared for presentation at the AIChE 2003 spring national meeting, New Orleans, LA; 2003.

[121] Visconti C, Tronconi E, Groppi G, Lietti L, Iovane M, Rossini S, et al. Monolithic catalysts with high thermal conductivity for the fischer-tropsch synthesis in tubular reactors. Chem Eng J 2011;171(3):1294–307.

[122] Hilmen A, Bergene E, Lindvåg O, Schanke D, Eri S, Holmen A. Fischer–Tropsch synthesis on monolithic catalysts with oil circulation. Catal Today 2005;105(3):357–61.

[123] de Deugd R, Kapteijn F, Moulijn J. Trends in Fischer–Tropsch reactor technology—opportunities for structured reactors. Top Catal 2003;26(1):29–39.

[124] Kapteijn F, de Deugd R, Moulijn J. Fischer–Tropsch synthesis using monolithic catalysts. Catal Today 2005;105(3):350–6.

[125] Hilmen A, Bergene E, Lindvåg O, Schanke D, Eri S, Holmen A. Fischer–Tropsch synthesis on monolithic catalysts of different materials. Catal Today 2001;69(1):227–32.

[126] Iglesia E, Reyes S, Madon R, Soled S. Selectivity control and catalyst design in the Fischer–Tropsch. Adv Catal 1993;39:221.

[127] van der Laan G. Kinetics, selectivity and scale up of the Fischer–Tropsch synthesis. University Library Groningen; 1999.

[128] Schulz H, Claeys M. Kinetic modelling of Fischer–Tropsch product distributions. Appl Catal A: Gen 1999;186(1):91–107.

[129] Donnelly T, Yates I, Satterfield C. Analysis and prediction of product distributions of the Fischer–Tropsch synthesis. Energy Fuels 1988;2(6):734–9.

[130] Satterfield C, Huff G. Carbon number distribution of Fischer–Tropsch products formed on an iron catalyst in a slurry reactor. J Catal 1982;73(1):187–97.

[131] Weller S, Friedel R. Isomer distribution in hydrocarbons from the Fischer–Tropsch process. J Chem Phys 1949;17:801.

[132] Dry ME. Practical and theoretical aspects of the catalytic Fischer–Tropsch process. Appl Catal A: Gen 1996;138(2):319–44.

[133] Bucher J. The effect of interference techniques on Fischer–Tropsch product distributions. [Ph.D. thesis]; 2010.

[134] Borg Ø, Dietzel P, Spjelkavik A, Tveten E, Walmsley J, Diplas S, et al. Fischer–Tropsch synthesis: cobalt particle size and support effects on intrinsic activity and product distribution. J Catal 2008;259(2):161–4.

[135] Escalona N, Medina C, Garcia R, Reyes P. Fischer Tropsch reaction from a mixture similar to biosyngas. Influence of promoters on surface and catalytic properties of CO/SiO_2 catalysts. Catal Today 2009;143(1):76–9.

[136] Klass D. Biomass for renewable energy and fuels. Encycl Energy 2004;1:193–212.

[137] Ledford H. Liquid fuel synthesis: making it up as you go along. Nature 2006;444(7120):677–8.

[138] Fargione J, Hill J, Tilman D, Polasky S, Hawthorne P. Land clearing and the biofuel carbon debt. Science 2008;319(5867):1235–8.

[139] Nanda S, Azargohar R, Dalai AK, Kozinski JA. An assessment on the sustainability of lignocellulosic biomass for biorefining. Renew Sustain Energy Rev 2015;50:925–41.

[140] Fleming JS, Habibi S, MacLean HL. Investigating the sustainability of lignocellulose-derived fuels for light-duty vehicles. Transp Res Part D: Transp Environ 2006;11(2):146–59.

[141] Jungbluth N, Büsser S, Frischknecht R, Tuchschmid M. Life cycle assessment of biomass-to-liquid fuels. Federal Office of Energy, Federal Office for the Environment, and Federal Office for Agriculture, Switzerland; 2008.

[142] Haase M, Skott S, Frohling M. Ecological evaluation of selected 1st and 2nd generation biofuel from wood and ethanol from sugar beets. In: Challenges for sustainable biomass utilisation: proceedings of the Chilean-German Biociclo workshop (Karlsruhe, 26.03. 2009); 2009.

[143] Yao Y, Hildebrandt D, Glasser D, Liu X. Fischer–Tropsch synthesis using H_2/CO/CO_2 syngas mixtures over a cobalt catalyst. Ind Eng Chem Res 2010;49(21):11061–6.

[144] Yao Y, Liu X, Hildebrandt D, Glasser D. The effect of CO_2 on a cobalt-based catalyst for low temperature Fischer Tropsch synthesis. Chem Eng J 2012;193:318–27.

[145] Srinivas S, Malik RK, Mahajani SM. Fischer–Tropsch synthesis using biosyngas and CO_2. Energy Sustain Dev 2007;11(4):66–71.

[146] White CM, Strazisar BR, Granite EJ, Hoffman JS, Pennline HW. Separation and capture of CO_2 from large stationary sources and sequestration in geological formations—coalbeds and deep saline aquifers. J Air Waste Manag Assoc 2003;53(6):645–715.

[147] Ni M, Leung MK, Leung DY, Sumathy K. A review and recent developments in photocatalytic water-splitting using TiO_2 for hydrogen production. Renew Sustain Energy Rev 2007;11(3):401–25.

[148] Maeda K, Teramura K, Lu D, Takata T, Saito N, Inoue Y, et al. Photocatalyst releasing hydrogen from water. Nature 2006;440(7082):295.

[149] Loges B, Boddien A, Junge H, Beller M. Controlled generation of hydrogen from formic acid amine adducts at room temperature and application in H_2/O_2 fuel cells. Angew Chem Int Ed 2008;47(2):3962–5.

[150] Klara SM, Srivastava RD. Us doe integrated collaborative technology development program for CO_2 separation and capture. Environ Prog 2002;21(4):247–53.

[151] Rochelle GT, et al. Amine scrubbing for CO_2 capture. Science 2009;325(5948):1652–4.

[152] MacDowell N, Florin N, Buchard A, Hallett J, Galindo A, Jackson G, et al. An overview of CO_2 capture technologies. Energy Environ Sci 2010;3(11):1645–69.

[153] Karadas F, Atilhan M, Aparicio S. Review on the use of ionic liquids (ils) as alternative fluids for CO_2 capture and natural gas sweetening. Energy Fuels 2010;24(11):5817–28.

[154] Abanades JC, Grasa G, Alonso M, Rodriguez N, Anthony EJ, Romeo LM. Cost structure of a postcombustion CO_2 capture system using CaO. Environ Sci Technol 2007;41(15):5523–7.

[155] Feron P, Hendriks C. CO_2 capture process principles and costs. Oil Gas Sci Technol 2005;60(3):451–9.

[156] Dry M. High quality diesel via the Fischer–Tropsch process—a review. J Chem Technol Biotechnol 2001;77(1):43–50.

[157] Swain PK, Das L, Naik S. Biomass to liquid: a prospective challenge to research and development in 21st century. Renew Sustain Energy Rev 2011;15(9):4917–33.

[158] Tijmensen M, Faaij A, Hamelinck C, van Hardeveld M. Exploration of the possibilities for production of Fischer Tropsch liquids and power via biomass gasification. Biomass Bioenergy 2002;23(2):129–52.

[159] Larson E, Jin H, Celik F. Large-scale gasification-based coproduction of fuels and electricity from switchgrass. Biofuels Bioprod Biorefin 2009;3(2):174–94.

[160] Ullah K, Sharma VK, Dhingra S, Braccio G, Ahmad M, Sofia S. Assessing the lignocellulosic biomass resources potential in developing countries: a critical review. Renew Sustain Energy Rev 2015;51:682–98.

[161] Boerrigter H. Economy of biomass-to-liquids (btl) plants. Energy Research Centre of the Netherlands (ECN). Available at: ⟨www ecn nl/publications⟩; 2006.

[162] Tock L, Gassner M, Maréchal F. Thermochemical production of liquid fuels from biomass: thermo-economic modeling, process design and process integration analysis. Biomass Bioenergy 2010;34(12):1838–54.

[163] Serrano-Ruiz J, Dumesic J. Catalytic production of liquid hydrocarbon transportation fuels. Catal Altern Energy Gener 2012:29.

[164] Borg Ø, Hammer N, Enger B, Myrstad R, Lindvåg O, Eri S, et al. Effect of biomass-derived synthesis gas impurity elements on cobalt Fischer–Tropsch catalyst performance including in situ sulphur and nitrogen addition. J Catal 2011;279(1):163–73.

[165] Göransson K, Söderlind U, He J, Zhang W. Review of syngas production via biomass dfbgs. Renew Sustain Energy Rev 2011;15(1):482–92.

[166] Asadullah M. Biomass gasification gas cleaning for downstream applications: a comparative critical review. Renew Sustain Energy Rev 2014;40:118–32.
[167] Blades T, Rudloff M, Schulze O. Sustainable sunfuel from chorens carbov® process. In: ISAF XV, San Diego; September 2005.
[168] Kamm B. Production of platform chemicals and synthesis gas from biomass. Angew Chem Int Ed 2007;46(27):5056–8.
[169] LeViness S, Deshmukh SR, Richard LA, Robota HJ. Velocys Fischer–Tropsch synthesis technology—new advances on state-of-the-art. Top Catal 2014;57 (6–9):518–25.
[170] Liu G, Yan B, Chen G. Technical review on jet fuel production. Renew Sustain Energy Rev 2013;25:59–70.
[171] Kim K, Kim Y, Yang C, Moon J, Kim B, Lee J, et al. Long-term operation of biomass-to-liquid systems coupled to gasification and Fischer–Tropsch processes for biofuel production. Bioresour Technol 2012;127:391–9.
[172] Hossain HZ, Hossain QH, Monir MMU, Ahmed MT. Municipal solid waste (msw) as a source of renewable energy in Bangladesh: revisited. Renew Sustain Energy Rev 2014;39:35–41.
[173] Tyagi VK, Lo SL. Sludge: a waste or renewable source for energy and resources recovery?. Renew Sustain Energy Rev 2013;25:708–28.
[174] Kalam MA, Hassan MH, bin Hajar R, bin Yusuf MS, bin Umar MR, Mahlia I. Palm oil diesel production and its experimental test on a diesel engine. In: Plant-based biofuels; 2008. p. 225 [chapter 16].
[175] Fontenelle A, Fernandes FA. Comprehensive polymerization model for Fischer–Tropsch synthesis. Chem Eng Technol 2011;34(6):963–71.
[176] de Klerk A, Furimsky E. Catalysis in the refining of Fischer–Tropsch syncrude. Platin Metals Rev 2011;55(4):263–7.
[177] James OO, Chowdhury B, Mesubi MA, Maity S. Reflections on the chemistry of the Fischer–Tropsch synthesis. RSC Adv 2012;2(19):7347–66.
[178] de Klerk A. Fischer-Tropsch facilities at a glance. In: Fischer–Tropsch Refining; 2011. p. 1–20.
[179] Khodakov AY, Chu W, Fongarland P. Advances in the development of novel cobalt Fischer–Tropsch catalysts for synthesis of long-chain hydrocarbons and clean fuels. Chem Rev 2007;107(5):1692–744.
[180] Maitlis PM, de Klerk A. Greener Fischer–Tropsch processes for fuels and feedstocks. John Wiley & Sons; 2013.
[181] Trippe F, Fröhling M, Schultmann F, Stahl R, Henrich E, Dalai A. Comprehensive techno-economic assessment of dimethyl ether (dme) synthesis and Fischer–Tropsch synthesis as alternative process steps within biomass-to-liquid production. Fuel Process Technol 2013;106:577–86.
[182] Swanson R, Platon A, Satrio J, Brown R. Techno-economic analysis of biomass-to-liquids production based on gasification. Fuel 2010;89:S11–9.
[183] Rudloff M. The choren btl process statusprogressfuture prospects. The RENEW ProjectRenewable Fuels for Advanced Powertrains, Integrated Project for Sustainable Energy Systems, Brussels; 2008.
[184] Kavalov B, Peteves S. Status and perspectives of biomass-to-liquid fuels in the European union. European CommissionDG JRC, Institute for Energy, Petten, The Netherlands 92-894; 2005.
[185] Yeh B. Independent assessment of technology characterizations to support the biomass program annual state-of-technology assessments. Contract 2011;303:275–3000.